molecular weight and that PLGA nanoparticles tended to release BP faster than PLA nanoparticles. The encapsulation efficiency of BP and BDP in nanoparticles prepared without zinc by the oil-in-water solvent diffusion method was lower (0.02 and 0.95 wt.%, respectively) than that of BP in nanoparticles prepared with zinc, as shown in Table 1. Therefore, nanoparticles encapsulating BDP (ca. 4 wt.%) prepared by the solvent evaporation method were used as the control for analysis of the steroid release profile. It was shown that the nanoparticles encapsulating BDP released more BDP within 5 days (Fig. 5). It has been reported that the glass-transition temperature (Tg) of a solid material obtained from PLGA and zinc oxide was higher than that of PLGA alone, presumably due to the formation of PLGA–zinc oxide complexes [15] and bivalent metal ions in microparticles delayed the degradation of PLGA through neutralization of acids liberated by the hydrolysis of PLGA [16–18]. Thus, the delayed release of BP observed in this study might have been induced by zinc.

On the other hand, BDP release from the nanoparticles prepared with PLGA (Mw 13,000) and PLA (Mw 14,000) showed little difference (data not shown), although BP release was strongly influenced by the composition of the polymers, as shown in Fig. 5. This suggests that BDP is distributed near the surface of the nanoparticles, while BP is distributed uniformly throughout the nanoparticles. Consequently, slower release of BP might also be induced by the difference of steroid distribution in the nanoparticles.

It is known that phagocytes accumulate in the inflammatory sites. Nanoparticles encapsulating a fluorescent dye (rhodamine) instead of BP, were incubated with murine macrophages, resulting in internalization of rhodamine encapsulated in the nanoparticles (Fig. 6A). This indicates that the nanoparticles were internalized in cells by phagocytosis as has been reported before [21]. The release of BP/BDP from macrophages after phagocytosis of the nanoparticles was also evaluated using BP-encapsu-

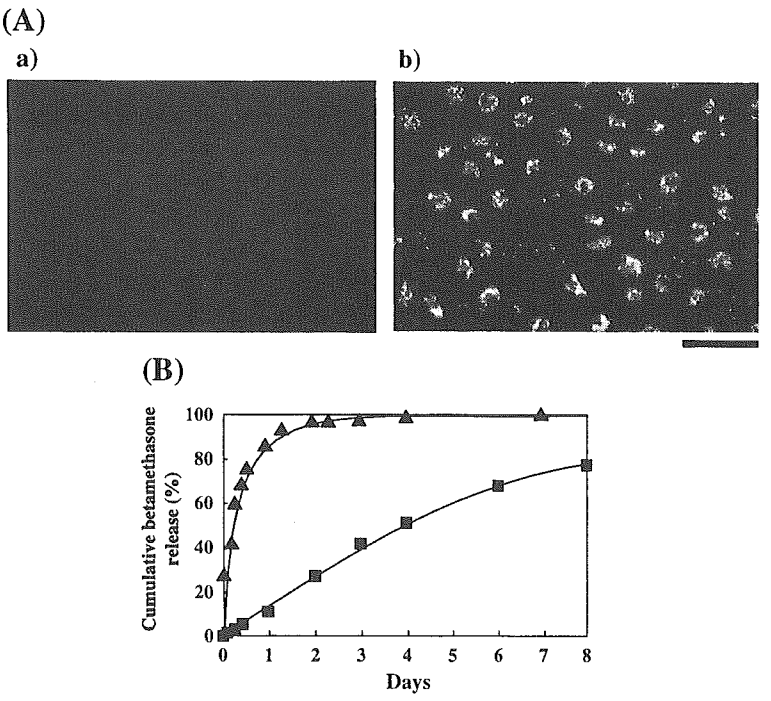

Fig. 6. (A) Fluorescence images of murine macrophages incubated with rhodamine (a) or rhodamine-encapsulated nanoparticles (b). Bar=50 μm. (B) Release of betamethasone from murine macrophages after phagocytosis of BP- (or BDP-) encapsulated nanoparticles. Nanoparticles were prepared with PLGA (Mw 8000) by the solvent diffusion method (■) or with PLA (Mw 14,000) by the solvent evaporation method (▲).

lated nanoparticles prepared according to the present method and BDP-encapsulated nanoparticles prepared by the solvent evaporation method. The BP-encapsulated nanoparticles showed continuous release of betamethasone for at least 8 days, while BDP-encapsulated nanoparticles released most of betamethasone after only 2 days (Fig. 6B). The sustained release of BP in diluted serum and from phagocytes, which are the main components of inflamed tissues, suggests that BP may be gradually released from nanoparticles at sites of inflammation in vivo.

4. Conclusions

Nanoparticles encapsulating betamethasone phosphate at a high efficiency were successfully prepared in the presence of zinc. It was found that zinc played a significant role in the formulation of nanoparticles. Zinc both increased the encapsulation efficiency of BP in the nanoparticles by formation of a water-insoluble complex with BP and influenced the formulation of the nanoparticles by interaction with a carboxyl group in the PLGA/PLA molecule. Sustained release of betamethasone from the nanoparticles suggested that zinc also slowed the degradation of PLGA/PLA. These nanoparticles had a diameter ranging from 80 to 250 nm, which is suitable for intravenous administration and accumulation in inflammatory sites. Moreover, BP was gradually released from murine macrophages in vitro. Overall, these results suggest that the nanoparticles might be developed as a novel anti-inflammatory agent with a long-term action on inflammatory sites in vivo.

Acknowledgements

The authors thank Sionogi and Co., Ltd. for supplying the TR-FIA assay kit. This work was supported by a grant for Research on Health Science Focusing on Drug Innovation from the Japan Health Science Foundation (KH63123). This work was also supported in part by a Health and Labour Sciences Research Grant from the Health and Labour Ministry of Japan (H14-Nano017).

References

[1] J.H. Senior, Fate and behavior of liposomes in vivo: a review of controlling factors, CRC Crit. Rev. Ther. Drug Carrier Syst. 3 (1987) 123–193.
[2] S.J. Douglas, S.S. Davis, L. Illum, Nanoparticles in drug delivery, CRC Crit. Rev. Ther. Drug Carrier Syst. 3 (1987) 233–261.
[3] Y. Mizushima, T. Hamano, K. Yokoyama, Tissue distribution and anti-inflammatory activity of corticosteroids incorporated in lipid emulsion, Ann. Rheum. Dis. 41 (1982) 263–267.
[4] Y. Mizushima, T. Hamano, K. Yokoyama, Use of a lipid emulsion as a novel carrier for corticosteroids, J. Pharm. Pharmacol. 34 (1982) 49–50.
[5] H. Okada, One- and three-month release injectable microspheres of the LH–RH superagonist leuprorelin acetate, Adv. Drug Deliv. Rev. 28 (1997) 43–70.
[6] H. Okada, Y. Doken, Y. Ogawa, H. Toguchi, Preparation of three-month depot injectable microspheres of leuprorelin acetate using biodegradable polymers, Pharm. Res. 11 (1994) 1143.
[7] T. Niwa, H. Takeuchi, T. Hino, N. Kunou, Y. Kawashima, Preparation of biodegradable nanospheres of water-soluble and insoluble drugs with D,L-lactide/glycolide copolymer by a novel spontaneous emulsification solvent diffusion method, and the drug release behavior, J. Control. Release 25 (1993) 89–98.
[8] Y. Kawashima, H. Yamamoto, H. Takeuchi, T. Hino, T. Niwa, Properties of a peptide containing DL-lactide/glycolide copolymer nanospheres prepared by novel emulsion solvent diffusion methods, Eur. J. Pharm. Biopharm. 45 (1998) 41–48.
[9] H. Murakami, M. Kobayashi, H. Takeuchi, Y. Kawashima, Preparation of poly(DL-lactide-co-glycolide) nanoparticles by modified spontaneous emulsification solvent diffusion method, Int. J. Pharm. 187 (1999) 143–152.
[10] E. Horisawa, T. Hirota, S. Kawazoe, J. Yamada, H. Yamamoto, H. Takeuchi, Y. Kawashima, Prolonged anti-inflammatory action of DL-lactide/glycolide copolymer nanospheres containing betamethasone sodium phosphate for an intra-articular delivery system in antigen-induced arthritic rabbit, Pharm. Res. 19 (2002) 403–410.
[11] S.P. Schwendeman, Recent advances in the stabilization of proteins encapsulated in injectable PLGA delivery systems, Crit. Rev. Ther. Drug Carr. Syst. 19 (2002) 73–98.
[12] X.M. Lam, E.T. Duenas, J.L. Cleland, Encapsulation and stabilization of nerve growth factor into poly(lactide-co-glycolic) acid microspheres, J. Pharm. Sci. 90 (2001) 1356–1365.
[13] G.P. Carino, J.S. Jacob, E. Mathiowitz, Nanosphere based oral insulin delivery, J. Control. Release 65 (2000) 261–269.
[14] X.M. Lam, E.T. Duenas, A.L. Daugherty, N. Levin, J.L. Cleland, Sustained release of recombinant human insulin-like growth factor-I for treatment of diabetes, J. Control. Release 67 (2000) 281–292.
[15] Y. Yamagata, M. Misaki, T. Kurokawa, K. Taira, S. Takada, Preparation of a copoly(DL-lactic/glycolic acid)–zinc oxide complex and its utilization to microcapsules containing recombinant human growth hormone, Int. J. Pharm. 251 (2003) 133–141.

[16] G. Zhu, S.R. Mallery, S.P. Schwendeman, Stabilization of proteins encapsulated in injectable poly(lactide-co-glycolide), Nat. Biotechnol. 18 (2000) 52–57.
[17] M.A. Tracy, K.L. Ward, L. Firouzabadian, Y. Wang, N. Dong, R. Qian, Y. Zhang, Factors affecting the degradation rate of poly(lactide-co-glycolide) microspheres in vivo and in vitro, Biomaterials 20 (1999) 1057–1062.
[18] X. Zhang, S. Zale, L. Sawyer, H. Bernstein, Effects of metal salts on poly(DL-lactide-co-glycolide) polymer hydrolysis, J. Biomed. Mater. Res. 34 (1997) 531–538.
[19] L.C. Makala, Y. Nishikawa, T. Kamada, H. Suzuki, X. Xuan, I. Igarashi, H. Nagasawa, Comparison of the accessory activity of murine peritoneal cavity macrophage derived dendritic cells and peritoneal cavity macrophages in a mixed lymphocyte reaction, J. Vet. Med. Sci. 63 (2001) 1271–1277.
[20] H. Okada, M. Yamamoto, T. Heya, Y. Inoue, S. Kamei, Y. Ogawa, H. Toguchi, Drug delivery using biodegradable microspheres, J. Control. Release 28 (1994) 121–129.
[21] M.E. Lutsiak, D.R. Robinson, C. Coester, G.S. Kwon, J. Samuel, Analysis of poly(D,L-lactic-co-glycolic acid) nanosphere uptake by human dendritic cells and macrophages in vitro, Pharm. Res. 10 (2002) 1480–1487.

Available online at www.sciencedirect.com

SCIENCE DIRECT®

Journal of Controlled Release 103 (2005) 93–98

journal of controlled release

www.elsevier.com/locate/jconrel

Drug-incorporating calcium carbonate nanoparticles for a new delivery system

Y. Ueno, H. Futagawa, Y. Takagi, A. Ueno, Y. Mizushima*

Institute of DDS, Jikei University School of Medicine, 3-25-8, Nishi-shinbashi, Minato-ku, Tokyo 105-8461, Japan

Received 7 July 2004; accepted 9 November 2004
Available online 15 December 2004

Abstract

We devised a simple method for incorporating drugs into solid calcium carbonate nanoparticles (nano-$CaCO_3$). The size of nano-$CaCO_3$ was controlled by mixing speed. Washing the nanoparticles released little incorporated drug but much drug that was adsorbed on the surface. In an in vitro releasing test, granulocyte colony-stimulating factor incorporated in nano-$CaCO_3$ was chemically stable and released very slowly. Subcutaneous injection of nano-$CaCO_3$ incorporating betamethasone phosphate (BP) resulted in a smaller initial increase in plasma concentration and a subsequent sustained release in compared with betamethasone phosphate solution. Nano-$CaCO_3$ may be useful to deliver hydrophilic drugs and bioactive proteins.

Keywords: Nanoparticle; Calcium carbonate; $CaCO_3$; DDS; Sustained release

1. Introduction

Many micro- and nanoparticles, mostly organic [1] and some inorganic [1,2] have been studied for the use in drug delivery systems (DDS). We developed a lipid nanoparticle of prostaglandin E_1 that has been used in clinic for last 15 years [3]. However, the use of drug incorporating $CaCO_3$ nanoparticles (nano-$CaCO_3$) has not been reported in DDS studies. Calcium carbonate ($CaCO_3$), calcium phosphate ($Ca(H_2PO_4)_2$), tricalcium phosphate ($Ca_3(PO_4)_2$) and hydroxyapatite ($Ca_5(PO_4)_3OH$) have been used in DDS [4,5]. Above all, $CaCO_3$ was reported to be useful as an intranasal carrier of insulin and hydrophilic compounds, because of its easy production and slow biodegradability [6–8]. In these reports, however, drugs or bioactive proteins were adsorbed on the surface of solid particles or porous $CaCO_3$ material. In these cases, the binding of the adsorbed drugs to $CaCO_3$ was not strong, which may result in insufficient sustained release or targeting.

In this study, we devised a simple method to incorporate hydrophilic drugs and bioactive proteins into nano-$CaCO_3$ and to regulate the size of the particles. The sustained release of drugs from the particles was confirmed both in vitro and in vivo experiments.

* Corresponding author. Tel.: +81 3 5733 7390; fax: +81 3 5733 7397.
E-mail address: mizushima@jikei.ac.jp (Y. Mizushima).

0168-3659/$ - see front matter © 2004 Elsevier B.V. All rights reserved.
doi:10.1016/j.jconrel.2004.11.015

2. Materials and methods

2.1. Materials

Erythropoietin and granulocyte-colony stimulating factor (G-CSF) were kind gifts from Chugai Pharmaceutical (Tokyo, Japan). Betamethasone sodium phosphate (BSP) was purchased from Sigma (St. Louis, MO). Male Sprague–Dawley rats were obtained from SLC Experimental Animals (Shizuoka, Japan) at 7 weeks of age. The body weights of rats at the time of experiments ranged from 186 to 230 g. The animal experiments were conducted in accordance with the Guide for the Care and Use of Laboratory Animals of Jikei University School of Medicine.

2.2. Incorporation and absorption of betamethasone phosphate into or on nano-CaCO3

Betamethasone phosphate (BP) was incorporated into calcium carbonate nanoparticles (nano-$CaCO_3$) by the following method: 650 μl of 5 M $CaCl_2$ and 375 μl of 5% BSP were gently mixed for 10 min, and then 2.5 ml of 1 M Na_2CO_3 was added and stirred gently or vigorously for 10 min. After the addition of 5 ml of distilled water and discarding the large particles of nano-$CaCO_3$ which were precipitated without centrifugation, the suspension was centrifuged (2000 rpm, 5 min) and the supernatant and precipitate were separated. The amount of BP in the supernatant and precipitate was measured respectively with HPLC, after dissolving the $CaCO_3$ with 0.5 M EDTA (pH 7.5). The fabricated nano-$CaCO_3$ containing BP were used for in vitro and in vivo experiments. We tested with different ratio in mole of $CaCl_2$/Na_2CO_3 at 1/1.6, 1/1.3, 1, 1.3, 1.6 and observed that the incorporation rate was highest at the ratio of 1.3, and used the ratio in this study.

To study the adsorption of BP, we mixed 650 μl of 5 M $CaCl_2$ and 2.5 ml of 1 M Na_2CO_3 and stirred gently or vigorously, according to desired particle size, and nano-$CaCO_3$ were formed. After the particles were washed with 5 ml of distilled water, 375 μl of 5% BSP was added and stirred to adsorb BP. The resulting suspension was centrifuged (2000 rpm, 5 min) and the amount of BP in the precipitate was determined by the method described above.

2.3. Incorporation and adsorption of erythropoietin in or on nano-CaCO3

Erythropoietin was incorporated into nano-$CaCO_3$ by mixing 650 μl of 5 M $CaCl_2$ and 125 μl of 1 mg/ml erythropoietin, and then by adding 2.5 ml of 1 M Na_2CO_3 stirring gently for 10 min at room temperature. After the addition of 5 ml of distilled water, the suspension was divided into two parts and centrifuged (2000 rpm, 5 min). One part was used for the measurement of erythropoietin, and the other part was washed by 0.9 ml of 1 M Na_2CO_3 twice to eliminate the adsorbed erythropoietin on the nano-$CaCO_3$. The both samples were dissolved by adding 1N HCl, and the amount of incorporated erythropoietin in the nano-$CaCO_3$ was measured with an ELISA kit (Toyobo, Osaka, Japan).

In the adsorption experiment with erythropoietin, 650 μl of 5 M $CaCl_2$ and 2.5 ml of 1 M Na_2CO_3 were mixed and stirred initially, and nano-$CaCO_3$ were formed. Next, the particles were washed by 5 ml of distilled water and 125 μl of 1 mg/ml erythropoietin was added and stirred to adsorb the erythropoietin. The resulting suspension was divided into two parts and centrifuged (2000 rpm, 5 min). The obtained precipitate of one part was used for the measurement of erythropoietin and that of the other part was washed twice by 0.9 ml of 1 M Na_2CO_3. The amount of erythropoietin of each part was determined by the method described above.

2.4. Particle size

Particle size of the prepared nano-$CaCO_3$ was measured with a laser light scattering method by using a fiber-optics particle analyzer (FPAR-1000, Otsuka Electronics, Osaka, Japan). The measurement was performed in triplicate, and the median size and range of distribution were obtained.

2.5. Release studies

2.5.1. Release of G-CSF from nano-CaCO3 preparation in vitro

To incorporate G-CSF in nano-$CaCO_3$, we mixed 650 μl of 5 M $CaCl_2$ and 250 μl of 500 μg/ml G-CSF, and added 2.5 ml of 1 M Na_2CO_3 stirring gently for 10 min. After the addition of 5 ml of distilled water,

the suspension was centrifuged (2000 rpm, 5 min) and the supernatant was discarded. The obtained precipitate was resuspended in 12.5 ml of 0.1 M Tris–HCl buffer (pH 7.2) containing 1% bovine serum albumin (final concentration of G-CSF was approximately 1 μg/ml) and shaken gently for 7 days at room temperature. For the measurement of G-CSF released from the preparations, 0.1 ml of the suspension was withdrawn and replaced with an equal volume of the same buffer. The samples were diluted and centrifuged (2000 rpm, 5 min) and amount of G-CSF in the obtained supernatant was measured with an ELISA kit (Immuno-Biological Laboratories, Gunma, Japan). These operations were carried out once a day for 7 days. After the final sampling on day 7, the total suspension was centrifuged and the precipitated nano-$CaCO_3$ were dissolved by adding 1N HCl and the residual amount of G-CSF was measured. A stability test on free G-CSF was also performed. Fifty μl of 100 μg/ml G-CSF and 4.95 ml of the same buffer were mixed (*final G-CSF concentration was 1.0 μg/ml*) and shaken simultaneously at room temperature. The amount of G-CSF in the solution (20 μl was taken) was measured with the ELISA kit once a day for 7 days.

2.5.2. Release of BP from nano-CaCO3 preparation in vivo

We administered 0.5 ml of the BP-incorporated nano-$CaCO_3$ suspension subcutaneously in rats at a dose of 1 mg/head. As a control, 0.5 ml of aqueous solution of BSP was administered subcutaneously in rats at a dose of 1 mg/head as BP. Blood was sampled via the inferior ophthalmic vein from rats anesthetized with ether before and 0.5, 1, 3, 5, 7, 16, 24 and 48 h after the administration. BP concentration in plasma was determined by a time-resolved fluoroimmunoassay.

2.6. Statistical analysis

The data derived from each experimental series are represented as the mean±S.E.M. The data were analyzed by using an ANOVA. Post-hoc determination were assessed for statistical significance by using Student's *t*-test [9].

3. Results

3.1. Loading (incorporation and absorption) of BP in or on nano-CaCO3 and particle size

Particle size and loading efficiency of nano-$CaCO_3$ were examined (Table 1). The diameter of the particles was dependent on mixing speed; gentle stirring (ca. 650 rpm) produced large particles, while vigorous stirring (ca. 1300 rpm) produced small particles. The range of distribution in particle size was narrower in the experiment with vigorous mixing than that with gentle one. The loading efficiency in particles of the both sizes was high and similar in the incorporation experiment. The BP contents in the supernatant by gentle and vigorous stirring was 8.9±1.7% and 9.4±1.3% of the total BP used, respectively. The amount of loading of BP in the adsorption experiment was much lower than that in the incorporation experiment.

3.2. Incorporation and adsorption of erythropoietin in or on nano-CaCO3

The diameter of the particles incorporating or adsorbing erythropoietin was 105.5±11.2 and 128.0±13.1 nm, respectively. The influence of washing on the release of erythropoietin was examined (Fig. 1). More adsorbed erythropoietin,

Table 1
Particle size of calcium carbonate nanoparticles (nano-$CaCO_3$) loading BP and their loading efficiency

Mixing speed	Particle size (nm)		Loading efficiency[a] (%)	
	Incorporation	Adsorption	Incorporation	Adsorption
Gentle ca. 650 rpm	140.7±21.4 (95.8–165.1)[b]	170.5±24.0 (139.5–209.5)	91.1±1.7	9.1±1.3
Vigorous ca. 1300 rpm	44.8±1.1 (35.3–56.8)	101.5±12.6 (80.9–131.7)	90.6±1.3	25.7±2.8

[a] Loading efficiency is the percentage of incorporated or adsorped BP compared to the total BP used. Each value represents mean±SEM of 3 experiment.
[b] Range of distribution in the particle size.

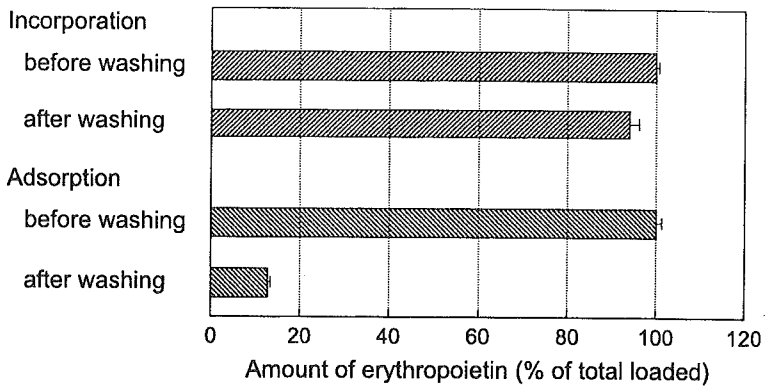

Fig. 1. Influence of washing on the release of drug from the calcium carbonate nanoparticles (nano-$CaCO_3$) either incorporating or adsorbing erythropoietin. The abscissa represents the percentage of erythropoietin content compared with that measured before washing. Each column and horizontal bar represents the mean±S.E.M. of three experiments.

compared to incorporated erythropoietin, was released after the particles were washed.

3.3. Sustained release of G-CSF from nano-CaCO3 preparation in vitro and stability of G-CSF in the particles and solution

The amount of G-CSF released over time from the nano-$CaCO_3$ was cumulatively plotted in Fig. 2. G-CSF was gradually released from the nano-$CaCO_3$ through 7 days and still remained in the nanoparticles on day 7. The amount (concentration) of G-CSF in the solution on day 7 was even smaller than that in the residue of the nano-$CaCO_3$, which indicated that G-CSF was not stable in the solution but was very stable in the nano-$CaCO_3$.

3.4. Sustained release of BP from nano-CaCO3 preparation in vivo

Plasma concentration of BP after the subcutaneous injection of BP-incorporated nano-$CaCO_3$ and free BP solution in rats is shown in Fig. 3. The nano-$CaCO_3$ used in the experiment were fabricated by gentle mixing. After the injection of BP solution, the plasma concentration of betamethasone was increased and

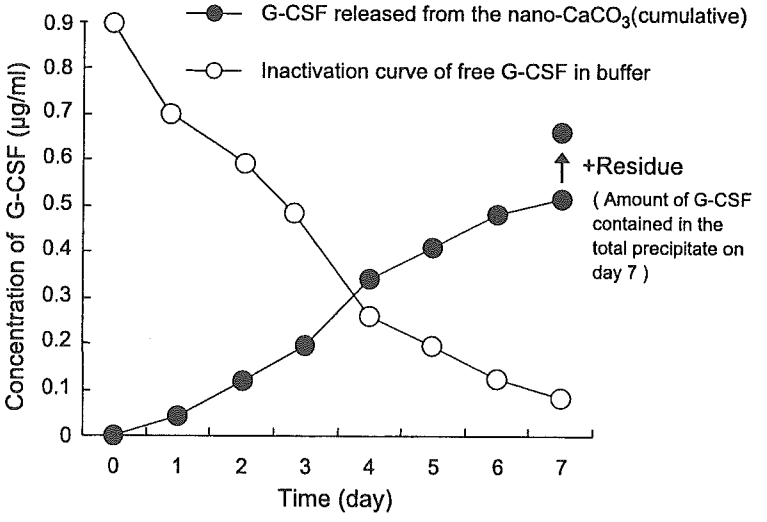

Fig. 2. In vitro release of granulocyte colony-stimulating factor (G-CSF) from calcium carbonate nanoparticles (nano-$CaCO_3$) (closed circle) and inactivation of free G-CSF in buffer (open circle). Each symbol represents the mean of three experiments.

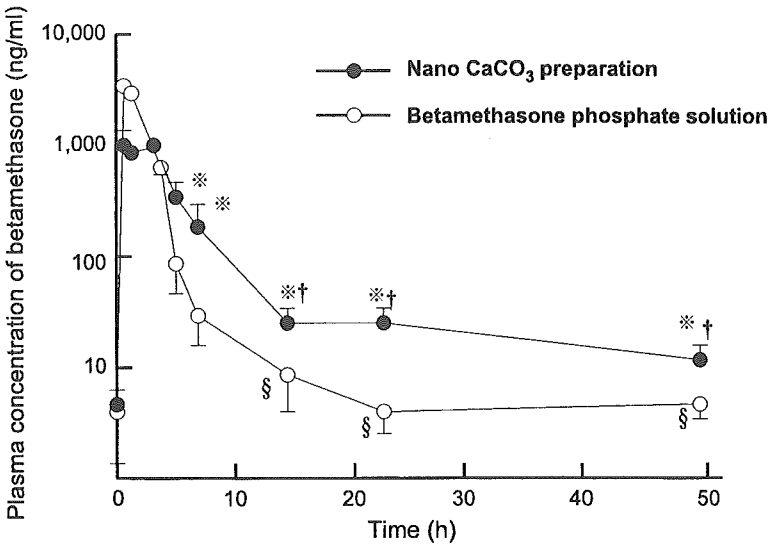

Fig. 3. Plasma concentration of betamethasone after the subcutaneous injection of calcium carbonate nanoparticles (nano-$CaCO_3$) incorporating BP (closed circle) and inactivation of free G-CSF in buffer (open circle). Each symbol represents the mean±S.E.M. of three experiments. ※: significant difference ($p<0.05$) between the two groups; †: significant difference ($p<0.05$) in relation to 0 h; §: no significant difference ($p>0.05$) in relation to 0 h.

then decreased steeply. While, after the injection of BP-incorporating nano-$CaCO_3$, the degree of initial increase in concentration was not high and a subsequent sustained release was observed in compared with the betamethasone solution. A significant sustained release was shown 48 h after the injection. However, an initial burst was observed even with the nano-preparation. It indicates that the release of BP from the nano-particles in subcutaneous tissue was rapid as compared with that in water (Table 1) even in the incorporated form.

4. Discussion

In the present study, we devised a simple method of incorporating drugs into nano-$CaCO_3$ that can be utilized for a delivery system. The incorporating efficiency of drugs was sufficiently high for the practical use in the clinic. It was confirmed in in vitro and in vivo experiments that the nano-$CaCO_3$ preparations showed a sustained release of incorporated drugs. Although the experimental reports of drug-adsorbing $CaCO_3$ particles have been published [6–8], the methods of incorporating drugs into $CaCO_3$ have not. The incorporated drugs are apparently more effective in DDS than the adsorbed drugs, because $CaCO_3$ particles are dissolved very slowly in the body.

In this study, we incorporated drugs with ionic, hydrophilic residues and low molecular weight, such as BP, and bioactive proteins, such as erythropoietin and G-CSF. Our preliminary experiments have shown this method of incorporating drugs to be practicable for low molecular weight compounds with a carboxyl residue, such as retinoic acid, those with a phosphate residue, such as hydrocortisone sodium phosphate, and those with a high molecular weight, such as immunoglobulin G and deoxyribonucleic acid (data not shown). Therefore, this method of incorporation is applicable to various drugs despite their molecular weight.

The diameters of nano-$CaCO_3$ incorporating BP were varied from 40 to 200 nm by changing the mixing speed (Table 1). Nanoparticles with a size of 50 or 200 nm have been reported to accumulate in angiogenic blood vessels [1,10], tumor [11] and inflamed tissues [3,12]. Thus, nano-$CaCO_3$ with incorporated anti-cancer and anti-inflammatory drugs may demonstrate targeting effects to the specific regions. We have obtained a preliminary result that nano-$CaCO_3$ accumulated in an inflamed region (data not shown). In addition, nanoparticles with a proper size and chemi-

cally appropriate surface properties were reported to penetrate the skin [13] and the blood–brain barrier [14].

Furthermore, the particles with the smallest size in this study (about 40 nm) should be able to avoid phagocytosis by the reticuloendothelial system (RES) or cells [1,15]. Avoiding clearance by the RES is very important in DDS using nanoparticles. Therefore, several attempts such as a modification of particle surface [16] and a use of surface binding of polyethyleneglycol (PEG) [2] were made.

The chemical stability of G-CSF was markedly increased with this incorporating method (Fig. 2). As well known, several bioactive proteins are unstable in the solution. We think that nano-$CaCO_3$ particles are also useful for the treatment with unstable bioactive proteins.

5. Conclusion

The present study describes a simple technology for incorporating drugs with low molecular weight and bioactive proteins into $CaCO_3$ nanoparticles, which can be used in various kinds of DDS.

Acknowledgements

Authors wish to appreciate Ministry of Health, Labour and Welfare of Japan for the Grant and Ms. M. Hara for her assistance in preparing the manuscript.

References

[1] N. Majeti, V.R. Kumar, Nano and microparticles as controlled drug delivery devices, J. Pharm. Pharm. Sci. 3 (2000) 234–258.
[2] M.E. Akerman, W.C. Chan, P. Laakkonen, S.N. Bhatia, E. Ruoslahti, Nanocrystal targeting in vivo, Proc. Natl. Acad. Sci. U. S. A. 99 (2002) 12617–12621.
[3] Y. Mizushima, Lipo-prostaglandin preparations, Prostaglandins Leukot. Essent. Fat. Acids 42 (1991) 1–6.
[4] M. Itokazu, T. Sugiyama, T. Ohno, E. Wada, Y. Katagiri, Development of porous apatite ceramic for local delivery of chemotherapeutic agents, J. Biomed. Mater. Res. 39 (1998) 536–538.
[5] W. Paul, C.P. Sharma, Ceramic drug delivery: a perspective, J. Biomater. Appl. 17 (2003) 253–264.
[6] S. Haruta, T. Hanafusa, H. Fukase, H. Miyajima, T. Oki, An effective absorption behavior of insulin for diabetic treatment following intranasal delivery using porous spherical calcium carbonate in monkeys and healthy human volunteers, Diabetes Technol. Ther. 5 (2003) 1–9.
[7] F. Ishikawa, M. Murano, M. Hiraishi, T. Yamaguchi, I. Tamai, A. Tsuji, Insoluble powder formulation as an effective nasal drug delivery system, Pharm. Res. 19 (2002) 1097–1104.
[8] A. Yanagawa, T. Kudo, Y. Mizushima, A novel particle carrier for transnasal peptide absorption, Jpn. J. Clin. Pharmacol. Ther. 26 (1995) 127–128.
[9] G.W. Snedecor, W.G. Cochran, The comparison of two samples, Statistical Methods, 8th ed., Iowa State University Press, Ames, 1989, pp. 83–106.
[10] J.D. Hood, M. Bednarski, R. Frausto, S. Guccione, R.A. Reisfeld, R. Xiang, D.A. Cheresh, Tumor regression by targeted gene delivery to the neovasculature, Science 296 (2002) 2404–2407.
[11] M. Takenaga, Application of lipid microspheres for the treatment of cancer, Adv. Drug Deliv. Rev. 20 (1996) 209–219.
[12] Y. Mizushima, T. Hamano, K. Yokoyama, Tissue distribution and anti-inflammatory activity of corticosteroids incorporated in lipid emulsion, Ann. Rheum. Dis. 41 (1982) 263–267.
[13] S. Miyazaki, A. Takahashi, W. Kubo, Poly *n*-butylcyanoacrylate (PNBCA) nanocapsules as a carrier for NSAIDs: in vitro release and in vivo skin penetration, J. Pharm. Pharm. Sci. 6 (2003) 238–245.
[14] P.R. Lockman, R.J. Mumper, M.A. Khan, D.D. Allen, Nanoparticle technology for drug delivery across the blood–brain barrier, Drug Dev. Ind. Pharm. 28 (2002) 1–13.
[15] M.A. Hossain, S. Maesaki, H. Kakeya, T. Noda, K. Yanagihara, E. Sasaki, Y. Hirakata, K. Tomono, T. Tashiro, S. Kohno, Efficacy of NS-718, a novel lipid nanosphere-encapsulated amphotericin B, against *Cryptococcus neoformans*, Antimicrob. Agents Chemother. 42 (1998) 66–4804.
[16] L. Araujo, R. Lobenberg, J. Kreuter, Influence of the surfactant concentration on the body distribution of nanoparticles, J. Drug Target. 6 (1999) 373–385.

Induction of Claudin-4 by Nonsteroidal Anti-inflammatory Drugs and Its Contribution to Their Chemopreventive Effect

Shinji Mima,[1] Shinji Tsutsumi,[1] Hironori Ushijima,[1] Miho Takeda,[1] Ikue Fukuda,[1] Kazumi Yokomizo,[1] Keitarou Suzuki,[1] Kuniaki Sano,[3] Tohru Nakanishi,[4] Wataru Tomisato,[2] Tomofusa Tsuchiya,[2] and Tohru Mizushima[1]

[1]Graduate School of Medical and Pharmaceutical Sciences, Kumamoto University, Kumamoto, Japan; [2]Faculty of Pharmaceutical Sciences and [3]Graduate School of Medicine and Dentistry, Okayama University and [4]Department of Clinical Pharmacy, Shujitsu University School of Pharmacy, Okayama, Japan

Abstract

Nonsteroidal anti-inflammatory drugs (NSAID) have shown chemopreventive effects in both preclinical and clinical studies; however, the precise molecular mechanism governing this response remains unclear. We used DNA microarray techniques to search for genes whose expression is induced by the NSAID indomethacin in human gastric carcinoma (AGS) cells. Among identified genes, we focused on those related to tight junction function (*claudin-4*, *claudin-1*, and *occludin*), particularly *claudin-4*. Induction of claudin-4 by indomethacin was confirmed at both mRNA and protein levels. NSAIDs, other than indomethacin (diclofenac and celecoxib), also induced claudin-4. All of the tested NSAIDs increased the intracellular Ca^{2+} concentration. Other drugs that increased the intracellular Ca^{2+} concentration (thapsigargin and ionomycin) also induced claudin-4. Furthermore, an intracellular Ca^{2+} chelator [1,2-bis(2-aminophenoxy)ethane-*N*,*N*,*N*′,*N*′-tetraacetic acid] inhibited the indomethacin-dependent induction of claudin-4. These results strongly suggest that induction of claudin-4 by indomethacin is mediated through an increase in the intracellular Ca^{2+} concentration. Overexpression of claudin-4 in AGS cells did not affect cell growth or the induction of apoptosis by indomethacin. On the other hand, addition of indomethacin or overexpression of claudin-4 inhibited cell migration. Colony formation in soft agar was also inhibited. Suppression of claudin-4 expression by small interfering RNA restored the migration activity of AGS cells in the presence of indomethacin. Based on these results, we consider that the induction of *claudin-4* and other tight junction–related genes by NSAIDs may be involved in the chemopreventive effect of NSAIDs through the suppression of anchorage-independent growth and cell migration. (Cancer Res 2005; 65(5): 1868-76)

Introduction

Nonsteroidal anti-inflammatory drugs (NSAID) are the most widely used therapeutic agents in the treatment of pain, inflammation, and fever (1). Recent epidemiologic studies clearly show that NSAID use is associated with a reduced risk of cancer, and preclinical and clinical studies have shown that some NSAIDs are effective for the treatment and prevention of cancer. This effect is particularly well documented in relation to colon and rectal cancer. Recent studies have also shown that NSAID use reduces the risk of stomach cancer (2, 3). Several different effects of NSAIDs on cancer cells, such as stimulation of apoptosis, cell growth suppression, inhibition of angiogenesis, and inhibition of metastasis, have been proposed to play important roles in NSAID-mediated chemoprevention (4, 5). However, the precise molecular mechanisms governing these effects of NSAIDs have not been elucidated.

The anti-inflammatory action of NSAIDs is mediated through its inhibition of cyclooxygenase (COX). COX is an enzyme essential for the synthesis of prostaglandins, which have a strong propensity for inducing inflammation. Prostaglandins, such as prostaglandin E_2 (PGE_2), inhibit apoptosis and stimulate cell growth, angiogenesis, and metastasis (6–8). Furthermore, overexpression of COX-2 (a subtype of COX) has been reported in various tumor cells and tissues (9, 10). Therefore, the inhibition of COX by NSAIDs was thought previously to be the sole explanation for their chemopreventive effect. However, several lines of evidence suggest that chemoprevention by NSAIDs also involves COX-independent mechanisms. Sulindac sulfone, a derivative of the NSAID sulindac, does not inhibit COX activity and has been shown to display antitumor activity *in vivo* as well as induce apoptosis and inhibit cell growth in tumor cells *in vitro* (11, 12). Moreover, the induction by NSAIDs of apoptosis and the inhibition of cell growth in COX-null fibroblasts and tumor cells in which COX expression was absent have been reported (13, 14). Therefore, it is important that the COX-independent mechanisms for chemoprevention by NSAIDs are elucidated to develop more effective NSAIDs.

Tight junctions are the most apical intercellular structure in epithelial and endothelial cells and create a physiologic barrier separating the apical and basolateral spaces; in other words, they create a paracellular permeability barrier. Tight junctions contain the transmembrane proteins occludin and claudin, which are connected to the cytoskeleton via zonula occludens (ZO-1; ref. 15). Several studies have shown a correlation between a reduction in tight junction function and tumor progression. A loss of tight junction structure is frequently observed in epithelium-derived cancers, whereas some tumor-promoting agents are known to disrupt tight junctions (16, 17). Furthermore, overexpression of tight junction–related proteins (such as claudin-1, claudin-4, and occludin) in cancer cells has been reported to induce apoptosis and suppress the invasive potential of these cells (18, 19).

NSAIDs affect the expression of several genes in a COX-independent manner. For example, NSAIDs induce NAG-1, a transforming growth factor-β superfamily member protein, which is involved in the induction of apoptosis by NSAIDs (20). We reported recently that NSAIDs induce CCAAT/enhancer binding protein homologous transcription factor, which is involved

Requests for reprints: Tohru Mizushima, Graduate School of Medical and Pharmaceutical Sciences, Kumamoto University, Kumamoto 862-0973, Japan. Phone: 81-96-371-4323; Fax: 81-96-371-4323; E-mail: mizu@gpo.kumamoto-u.ac.jp.

in the induction of apoptosis by endoplasmic reticulum stressors. By using a CCAAT/enhancer binding protein homologous transcription factor–deficient mouse, we showed that this induction is essential for NSAID-induced apoptosis (21). Therefore, systematic screening of genes whose expression is induced by NSAIDs is important for understanding the COX-independent mechanism of chemoprevention by NSAIDs. In this study, we searched for genes in human gastric carcinoma (AGS) cells whose expression is induced by indomethacin. We found that claudin-4, claudin-1, and occludin were induced in these cells in the presence of indomethacin. We propose that the induction of claudin-4 is mediated by an increase in the intracellular Ca^{2+} concentration. Moreover, by using claudin-4-overexpressing cells and small interfering RNA (siRNA), we show that claudin-4 is involved in the NSAID-mediated suppression of anchorage-independent growth and cell migration.

Materials and Methods

Chemicals and Media. Ham's F-12 and RPMI 1640 were purchased from Nissui Pharmaceutical Co. (Tokyo, Japan). Fetal bovine serum was purchased from Life Technologies (Tokyo, Japan). 1,2-Bis(2-aminophenoxy)ethane-*N*,*N*,*N*′,*N*′-tetraacetic acid was purchased from Dojindo Co. (Tokyo, Japan). Thapsigargin, ionomycin, G418, 3-(4,5-dimethylthiazol-2-yl)-2,5-diphenyltetrazolium bromide, diclofenac, and cycloheximide were purchased from Sigma Co. (Tokyo, Japan). Indomethacin, *N*-acetylcysteine, and superoxide dismutase (SOD) were from Wako Co. (Tokyo, Japan). Celecoxib was purchased from LKT Laboratories, Inc. (St. Paul, MN). Antibodies against claudin-4 and actin were purchased from Santa Cruz Biotechnology, Inc. (Santa Cruz, CA).

Cell Culture and Overexpression of Claudin-4. AGS cells were cultured in Ham's F-12 medium containing 10% fetal bovine serum. Other cell types (MKN-45, KATO-III, Caco-2, and HCT-15) were cultured in RPMI 1640 containing 10% fetal bovine serum. Cells (2×10^5 per well in a 24-well plate) were cultured for 24 hours and used in the experiments. Cell viability was determined by the 3-(4,5-dimethylthiazol-2-yl)-2,5-diphenyltetrazolium bromide method as described previously (22).

A full-length human claudin-4 cDNA was PCR amplified from the cDNA of AGS cells and cloned into pcDNA3.1(-) (Invitrogen, Carlsbad, CA). Transfection of AGS cells with plasmids was carried out using Lipofectamine 2000 (Invitrogen) according to the manufacturer's protocols. The stable transfectants expressing claudin-4 were selected by immunoblotting analysis. Positive clones were maintained in the presence of 300 μg/mL G418.

DNA Microarray Analysis. Total RNA was extracted from cells treated with 0.3 mmol/L indomethacin for 4 hours or nontreated cells using a RNeasy kit (Qiagen, Hilden, Germany) according to the manufacturer's protocols. Samples (10 μg RNA) were labeled with cyanine 3– or cyanine 5–conjugated dUTP with the use of an Agilent cDNA labeling kit. The fluorescent-labeled cDNAs were mixed and hybridized simultaneously to Agilent cDNA microarray human I. The microarray was scanned with a DNA Microarray Scanner (Agilent, Palo Alto, CA) using laser excitation at 532 and 635 nm wavelengths for the cyanine 3 and cyanine 5 labels, respectively. The raw pixel intensity images were analyzed using the Feature Extraction and Analysis Software version 7.5 (Agilent). After pixel intensity determination and background subtraction, the ratio of the intensity of the treated cells to the intensity of the control was calculated following normalization.

Reverse Transcription. Total RNA was extracted from cells using a RNeasy kit according to the manufacturer's protocols. Samples (10 μg RNA) were reverse transcribed using a first-strand cDNA synthesis kit (Amersham, Tokyo, Japan) according to the manufacturer's instructions. For traditional reverse transcription–coupled PCR (RT-PCR), synthesized cDNA was amplified by PCR [Takara (Shiga, Japan) PCR Thermal Cycler] using KOD Plus Polymerase (Toyobo, Osaka, Japan), and reaction products were analyzed by agarose gel electrophoresis. For real-time RT-PCR, synthesized cDNA was applied to real-time RT-PCR (ABI PRISM 7700) using SYBR Green PCR Master Mix (ABI) and analyzed with ABI PRISM 7700 Sequence Detection Software according to the manufacturer's instructions. Real-time cycle conditions were 2 minutes at 50°C followed by 10 minutes at 90°C and then for 45 cycles at 95°C for 30 seconds and 63°C for 60 seconds. Specificity was confirmed by electrophoretic analysis of the reaction products and by inclusion of template-free or reverse transcriptase–free controls. To normalize the amount of total RNA present in each reaction, *GAPDH* or *actin* genes were used as an internal standard.

Primer Design. Primers were designed using the Primer3 Web site (http://frodo.wi.mit.edu/cgi-bin/primer3/primer3_www.cgi). Primers are listed as gene name, forward primer, reverse primer. For RT-PCR: *claudin-1*, CCGTTGGCATGAAGTGTATG, CCAGTGAAGAGAGCCTGACC; *claudin-4*, CTCTGTGGCCTCAGGACTCT, CAGGACTTCCAAGGGTGAAG; *occludin*, TCCAATGGCAAAGTGAATGA, GCAGGTGCTCTTTTTGAAGG; *COX-1*, CTGGCTCCGGAATTCACT, CATCTGGCAACTGCTTCTTC; *COX-2*, CCACCAACTTACAATGCTGC, CACCAGACCAAAGACCTCC; and *actin*, GGACTTCGAGCAAGAGATGG, AGCACTGTGTTGGCGTACAG. For PCR cloning: *claudin-4*, CGGGATCCCTGACAATGGCCTCCATGGGGCT, GCTCTAGATTACACGTAGTTGCTGGCAGC.

Immunoblotting and Northern Blotting Analyses. Whole cell extracts were prepared as described previously (23). The protein concentration of samples was determined by the Bradford method. Samples were applied to 12% SDS-PAGE gels and subjected to electrophoresis, and proteins were then immunoblotted with respective antibodies.

Total RNA was extracted from the cells using a RNeasy kit according to the manufacturer's protocols. Samples (5 μg RNA) were separated by agarose (1%) gel electrophoresis in the presence of 6.3% formaldehyde and blotted onto nylon membranes. DNA probes for claudin-4 were amplified by PCR and labeled with [α-^{32}P]dCTP (6,000 Ci/mmol, Amersham) using the Rediprime II DNA Labeling System (Amersham) according to the manufacturer's instructions. After hybridization and washing, membranes were analyzed with BAS2000A (Fujix, Kanagawa, Japan).

Measurement of the Intracellular Ca^{2+} Concentration, $[Ca^{2+}]_i$. The intracellular Ca^{2+} concentration, $[Ca^{2+}]_i$, was monitored according to manufacturer's protocols (24). Cells were washed with assay buffer containing 115 mmol/L NaCl, 5.4 mmol/L KCl, 1.8 mmol/L $CaCl_2$, 0.8 mmol/L $MgCl_2$, 20 mmol/L HEPES, and 13.8 mmol/L glucose. Cells were then incubated with 4 μmol/L fluo-3/AM in the assay buffer containing 0.1% bovine serum albumin, 0.04% Pluronic F127, and 2 mmol/L probenecid for 40 minutes at 37°C. After washing twice with the assay buffer, cells were suspended in assay buffer containing 2 mmol/L probenecid. Fluo-3 fluorescence of cells in a water-jacketed cuvette (1.6×10^6 cells per cuvette) was measured with a Hitachi (Tokyo, Japan) F-4500 spectrofluorophotometer by recording excitation signals at 490 nm and the emission signal at 530 nm at 1-second intervals. Maximum and minimum fluorescence values (F_{max} and F_{min}) were obtained by adding 10 mol/L ionomycin and 10 mol/L ionomycin plus 5 mmol/L EGTA (in Ca^{2+}-free medium), respectively. $[Ca^{2+}]_i$ was calculated according to the following equation: $[Ca^{2+}]_i = K_d(F - F_{min}) / (F_{max} - F)$, where K_d is the apparent dissociation constant (400 nmol/L) of the fluorescence dye-Ca^{2+} complex (24).

Cell Migration Assays. *In vitro* wound healing assays were used to assess cell migration as described previously (25). Confluent AGS cells on a 24-well plate were used. Two linear wounds were scratched with a p200 pipette tip. The cell-free area was measured before and after 24 hours of incubation (healing step) using Scion Image software (Scion Corp., Frederick, MD).

Soft Agar Assay. Soft agar assay was done as described previously (26). Cells (2×10^4 per dish) were suspended in 0.5 mL of 0.3% Noble agar (Difco, Detroit, MI) supplemented with complete culture medium. This suspension was layered over 0.5 mL of a 0.8% agar medium base layer in 35 mm culture dishes (Iwaki, Chiba, Japan). After 10 days, cells were stained with crystal violet and colonies were counted.

siRNA Targeting of Claudin-4. Synthetic siRNAs were purchased from Qiagen. The target DNA sequence of claudin-4 is CCCGCACAGACAAGCCTTACT and siRNA 5′-CGCACAGACAAGCCUUACUUU-3′ and 5′-AGUAAGGCUUGUCUGUGCGGG-3′ were used as annealed oligonucleotides. AGS cells were transfected with siRNA using RNAiFect Transfection Reagent (Qiagen) according to the manufacturer's instructions.

Statistical Analysis. All values are expressed as mean ± SE. One-way ANOVA followed by Scheffe's multiple comparison test was used for evaluation of differences between the groups. The Student's *t* test for unpaired results was done for the evaluation of differences between two groups, which were considered to be significant for values of $P < 0.05$.

Results

DNA Microarray Analysis for Gene Expression in the Presence of Indomethacin. We used the DNA microarray technique and AGS cells to identify genes whose expression is altered by indomethacin. AGS cells were treated with 0.3 mmol/L indomethacin for 4 hours before microarray analysis. As shown in Fig. 1*A*, this treatment did not affect cell viability. We did microarray analysis four times (four hybridizations) and selected genes that were induced by indomethacin based on the criteria that the induction was observed in all four hybridizations and that the mean value (fold change) of four hybridizations was >2.0. As shown in Table 1, 34 genes were identified. Induction of some of these genes, such as *CCAAT/enhancer binding protein* β and *prostate differentiation factor* (*NAG-1*), by NSAIDs in other cancer cell types has been reported previously (20, 27). Among these genes, we focused our attention on genes related to tight junction function (*claudin-1*, *claudin-4*, and *occludin*), particularly on *claudin-4*, because the induction was relatively clear, its expression in gastric mucosal cells has been confirmed previously (28), and a recent report showed that overexpression of claudin-4 suppressed anchorage-independent growth and the invasive potential of pancreatic cancer cells (19). Nineteen genes were identified whose expression was repressed by the indomethacin treatment (data not shown).

Changes in the indomethacin-induced expression of these genes were then verified by RT-PCR. As shown in Fig. 1*B*, the induction of claudin-1, claudin-4, and occludin was confirmed. Results of the

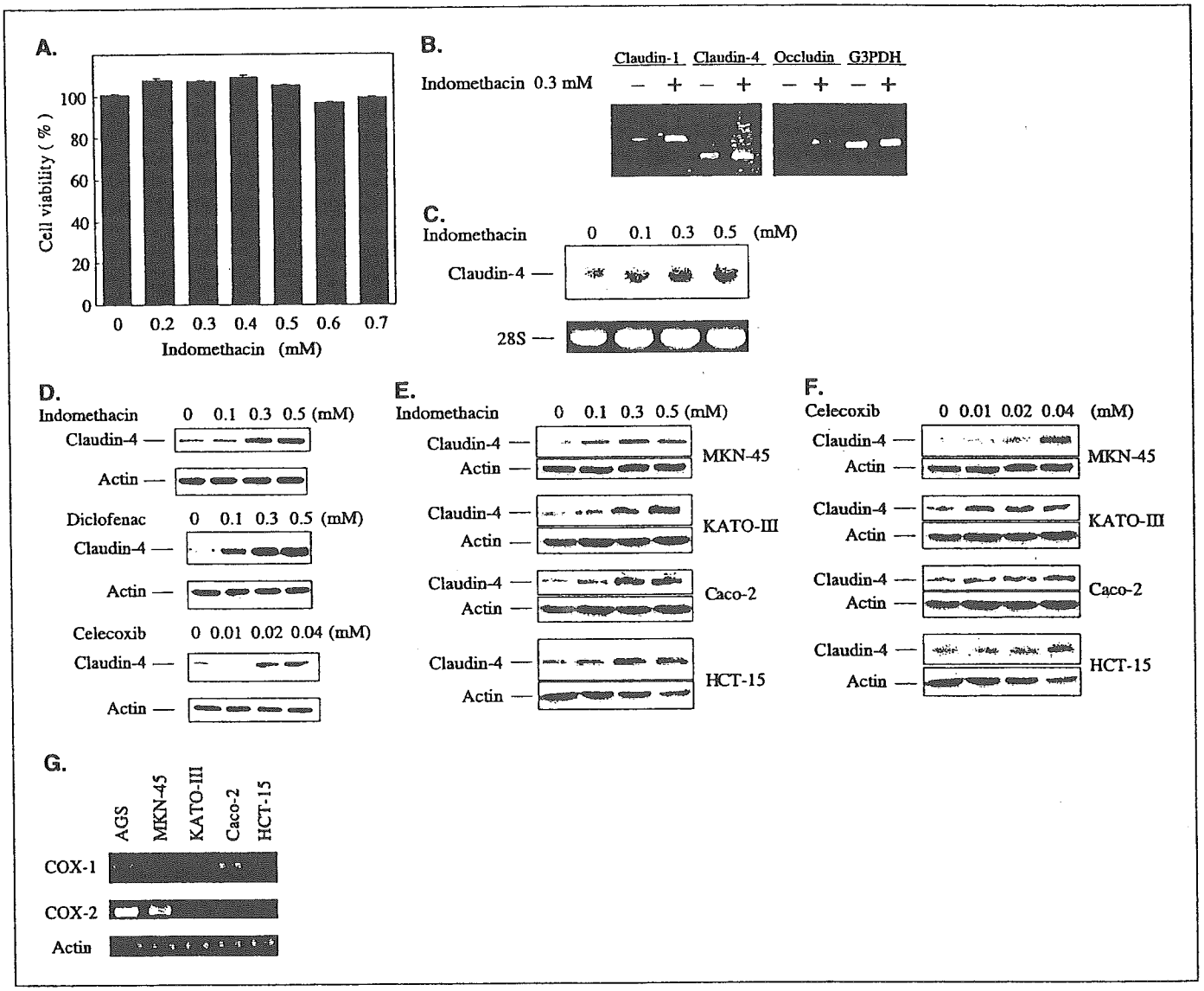

Figure 1. Induction of tight junction–related genes by NSAIDs. AGS (*A-D* and *G*) or MKN-45, KATO-III, Caco-2, and HCT-15 (*E-G*) cells were incubated with indicated concentrations of NSAIDs for 4 hours (*A-C*) or 24 hours (*D-F*). Results for cells cultured without NSAIDs (*G*). Cell viability was determined by the 3-(4,5-dimethylthiazol-2-yl)-2,5-diphenyltetrazolium bromide method. *Columns*, mean ($n = 3$); *bars*, SE (*A*). Total RNA was extracted and subjected to RT-PCR by use of a specific primer for each gene. GAPDH (*G3PDH*; *B*) or actin (*G*) was used as a control. Reaction products were analyzed by agarose (1%) gel electrophoresis (*B* and *G*). Total RNA samples were analyzed by Northern blotting experiments using a specific DNA probe for claudin-4. Bands of rRNA (28S) stained with ethidium bromide (*C*). Whole cell extracts (2.5 μg protein) were analyzed by immunoblotting with an antibody against claudin-4 or actin (*D-F*).

Table 1. List of genes overexpressed in AGS cells following treatment with indomethacin

Gene name	Accession no.	Function	Fold change
Claudin-1	AF115546	Tight junction	2.00
Claudin-4	AK026651	Tight junction	2.54
Occludin	U49184	Tight junction	2.24
Tissue factor pathway inhibitor 2	NM_006528	Blood coagulation	2.46
Zinedin	AF212940	Calmodulin binding protein	2.01
Arginine-rich protein	AA582041	Carcinogenicity	2.00
Human urokinase-type plasminogen receptor, exon 7	U09937	Cell surface plasminogen activation	2.81
Chromobox homologue 4 (Drosophila Pc class)	AF013956	Cellular memory system	2.30
Human low-density lipoprotein receptor gene, exon 18	L00352	Cholesterol homeostasis	3.43
Low-density lipoprotein receptor (familial hypercholesterolemia)	NM_000527	Cholesterol homeostasis	2.75
Epithelial protein lost in neoplasm β	AA594624	Cytoskeleton	2.58
Keratin 8	AI978932	Cytoskeleton	2.37
Immediate early response 3	AI022951	Differentiation	2.36
Prostate differentiation factor	AB000584	Differentiation	2.00
Procollagen-proline	J02783	Disulfide isomerase/oxidoreductase	2.50
Glucosidase β, acid (includes glucosylceramidase)	AF023268	Glucocerebrosidase	2.01
Tumor necrosis factor--induced protein 6	M31165	Hyaluronan binding protein family	2.14
Basigin	X64364	Immunoglobulin superfamily	2.15
Solute carrier family 7	M80244	L-Amino acid transporter	3.00
Cathepsin D	M11233	Lysosomal proteinase	2.40
Pim-1 oncogene	M24779	Protein kinase	2.52
Cytochrome c oxidase subunit VIII	J04823	Respiratory	2.90
3,4-Dihydroxy-L-phenylalanine decarboxylase (aromatic l-amino acid decarboxylase)	M76180	Synthesis of dopamine and serotonin	2.27
CCAAT/enhancer binding protein β	W93514	Transcription factor	4.76
Predicted using Genefinder, preliminary prediction	CAB60892	Tumor protein p53	2.18
ATPase, H^+ transporting, lysosomal (vacuolar proton pump) 21 kDa	AI567477	Vacuolar proton pump	2.39
Ribosomal protein S21	BE221408	Unknown	2.34
Human genomic DNA, chromosome 22q11.2, BCRL2 region	AP000553	Unknown	2.23
Ubiquinol-*cytochrome c* reductase (6.4 kDa) subunit	AW163002	Unknown	2.13
IFN-induced transmembrane protein 3 (1-8U)	X57352	Unknown	2.10
Conserved hypothetical protein	AAF96700	Unknown	2.07
KIAA0316 gene product	AB002314	Unknown	2.06
Sequence 100 from patent WO9951727	AX015425	Unknown	2.03
Ribosomal protein S28	AW161288	Unknown	2.03

NOTE: Fold changes in gene expression by indomethacin compared with untreated cells. Mean values from four independent hybridizations. AGS cells were treated with or without 0.3 mmol/L indomethacin for 4 hours and subjected to DNA microarray analysis.

real-time RT-PCR experiments used to determine the extent of the induction yielded fold changes in copy number of 2.3, 3.0, and 1.5 for claudin-1, claudin-4, and occludin mRNA, respectively, in response to treatment of cells for 4 hours with 0.3 mmol/L indomethacin. In addition, the induction by indomethacin of claudin-4 mRNA or claudin-4 protein was confirmed using Northern blot analysis (Fig. 1*C*) and immunoblot analysis (Fig. 1*D*), respectively.

We then examined whether the induction of claudin-4 by indomethacin is specific to AGS cells or is a general property also observed in other cell types. We used MKN-45 and KATO-III cells (derived from gastric cancer tissue) and Caco-2 and HCT-15 cells (derived from colon cancer tissue) to test this effect. As shown in Fig. 1*E*, indomethacin induced claudin-4 in each of the cell lines tested, with the concentration of indomethacin required for the induction being similar for each cell line.

Diclofenac, another NSAID, also induced claudin-4 in a dose-dependent manner (Fig. 1*D*). Some NSAIDs are specific in their effect on COX, which exists in two forms, COX-1 and COX-2. Celecoxib, a COX-2-specific NSAID, induced claudin-4 not only in AGS cells (Fig. 1*D*) but also in the other cell lines tested (Fig. 1*F*). These results suggest that NSAIDs induce claudin-4 irrespective of whether they are specific for COX-2. It has been reported that both COX-1 and COX-2 mRNA are expressed in AGS, MKN-45, and Caco-2 cells, whereas COX-2 mRNA expression is very low in KATO-III and HCT-15 cells (29–33). COX-1 mRNA expression was confirmed by RT-PCR in each of the cell lines tested, whereas COX-2 mRNA expression was detected only in AGS, MKN-45, and Caco-2 cells (Fig. 1*G*). Therefore, COX-2-specific NSAIDs (in this case, celecoxib) induce claudin-4 not only in COX-2-expressing cells but also in cells lacking COX-2 expression. Furthermore, whereas indomethacin inhibited both COX-1 and COX-2 at a concentration of <1 nmol/L (34), the induction of claudin-4 required higher concentrations (Fig. 1). These findings strongly suggest that NSAIDs induce claudin-4 independently of COX-inhibition.

Mechanism for Induction of Claudin-4 by Indomethacin. For further confirmation that NSAIDs induce claudin-4 independently of COX-inhibition, we examined the effect of PGE_2, a major prostaglandin in the gastric mucosa, on the induction of claudin-4

by indomethacin. PGE_2 (0.1-10 μmol/L) did not affect the level of claudin-4 in the presence and absence of indomethacin (Fig. 2*A*). We determined previously the level of PGE_2 in the culture medium of AGS cells to be ~10 nmol/L (23). Therefore, inhibition of PGE_2 synthesis by indomethacin does not seem to be involved in the induction of claudin-4 by indomethacin.

Recent studies suggest that indomethacin and other NSAIDs act as agonists of the peroxisome proliferator-activated receptor-γ (35). To test the contribution of this activity to the induction of claudin-4 by indomethacin, we examined the effect of a peroxisome proliferator-activated receptor-γ antagonist (GW9662) on the induction of claudin-4 by indomethacin. As shown in Fig. 2*B*, GW9662 did not inhibit but rather slightly heightened the induction of claudin-4 by indomethacin. The different concentrations of GW9662 tested did not affect cell viability (data not shown), but based on data from a previous report, these concentrations are considered sufficient to inhibit agonist binding to peroxisome proliferator-activated receptor-γ (36). Therefore, peroxisome proliferator-activated receptor-γ does not seem to be associated with the induction of claudin-4 by indomethacin.

It has been reported that some NSAIDs increase reactive oxygen species production (37). To test the contribution of reactive oxygen species to the induction of claudin-4 by indomethacin, we examined the effects of the antioxidants *N*-acetylcysteine and SOD. As shown in Fig. 2*C* and *D*, neither *N*-acetylcysteine nor SOD affected claudin-4 expression in either the presence or the absence of indomethacin. Activation of the extracellular signal-regulated kinase pathway—one of the mitogen-activated protein kinase pathways—has been reported to stimulate the expression of claudin-4. Although some NSAIDs have been reported to activate the extracellular signal-regulated kinase pathway (19, 38), an inhibitor of extracellular signal-regulated kinase (PD98059) did not affect the expression of claudin-4 in either the presence or the absence of indomethacin (Fig. 2*E*). *N*-acetylcysteine, SOD, and PD98059 did not affect cell viability at the concentrations used (data not shown). These results suggest that neither reactive oxygen species nor extracellular signal-regulated kinase is responsible for the induction of claudin-4 by indomethacin.

Some NSAIDs have been reported to increase the intracellular Ca^{2+} concentration, $[Ca^{2+}]_i$ (39, 40). In this study, we tested whether an increase in $[Ca^{2+}]_i$ by NSAIDs is responsible for the induction of claudin-4. Firstly, we confirmed that a NSAID-induced increase in $[Ca^{2+}]_i$ occurred under the same conditions as those in which the induction of claudin-4 in AGS cells was observed. As shown in Fig. 3*A*, all NSAIDs tested (indomethacin, diclofenac, and celecoxib) increased $[Ca^{2+}]_i$ at the same NSAID concentrations that caused the induction of claudin-4.

Some drugs that are known to increase $[Ca^{2+}]_i$ were examined for their capacity to induce claudin-4 expression. The actions of thapsigargin, an inhibitor of the sarcoplasmic/endoplasmic reticulum Ca^{2+} ATPase, and the Ca^{2+} ionophore ionomycin were thus tested on AGS cells. As shown in Fig. 3*A-C*, in addition to increasing $[Ca^{2+}]_i$, both thapsigargin and ionomycin induced claudin-4 in a dose-dependent manner. Furthermore, an intracellular Ca^{2+} chelator, 1,2-bis(2-aminophenoxy)ethane-*N,N,N',N'*-tetraacetic acid, was found to inhibit the induction of claudin-4 not only by ionomycin but also by indomethacin (Fig. 3*D*). 1,2-Bis(2-aminophenoxy)ethane-*N,N,N',N'* -tetraacetic acid did not affect cell viability at the concentration used in these experiments (data not shown). These results strongly suggest that induction of claudin-4 by indomethacin is mediated via an increase in $[Ca^{2+}]_i$.

Role of Claudin-4 Induction in the *In vitro* Antitumor Action of NSAIDs. As described in Introduction, various mechanisms have been proposed for the chemopreventive action of NSAIDs; these include the inhibition of cell growth, stimulation of

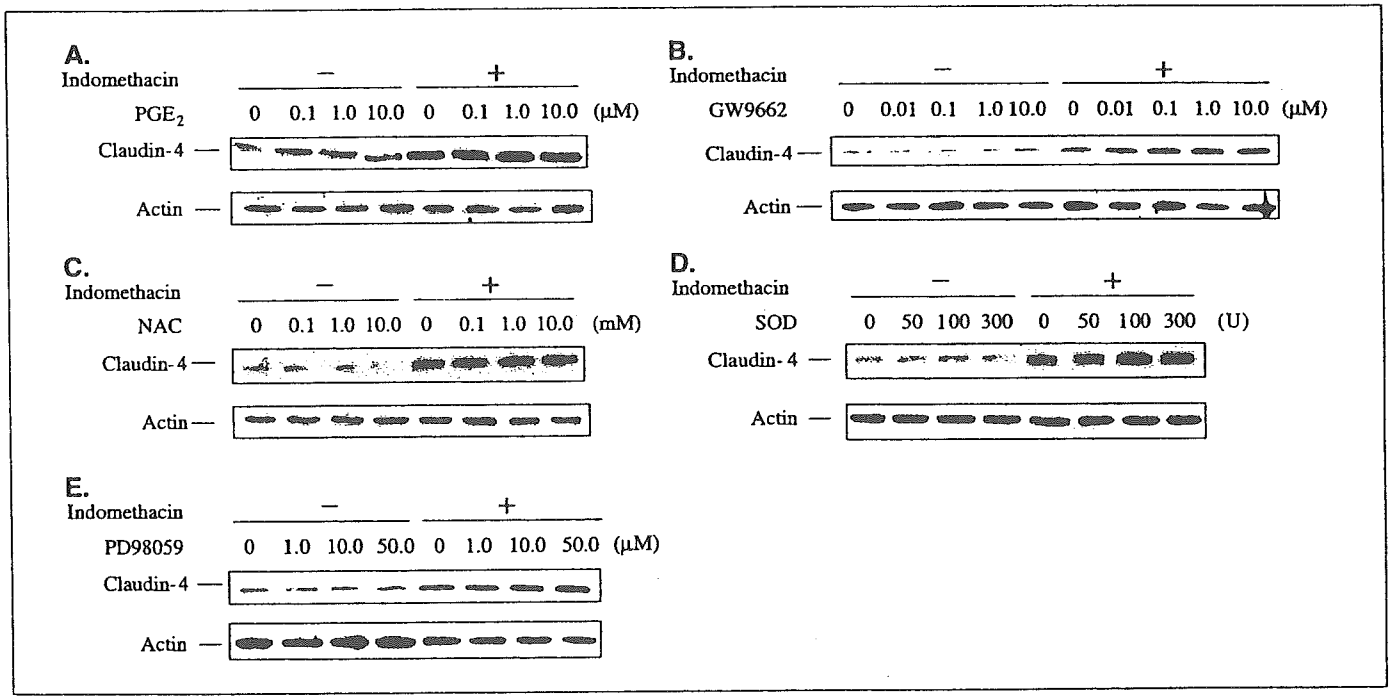

Figure 2. Mechanism for the induction of claudin-4 by indomethacin. AGS cells were incubated with or without 0.3 mmol/L indomethacin for 24 hours in the presence of indicated concentrations of PGE_2 (*A*), GW9662 (*B*), *N*-acetylcysteine (*NAC*; *C*), SOD (*D*), or PD98059 (*E*). Levels of claudin-4 and actin were estimated by immunoblotting experiments as described in Fig. 1. One unit of SOD was evaluated based on its inhibitory effect on the reduction of cytochrome *c* as described in the manufacturer's instructions.

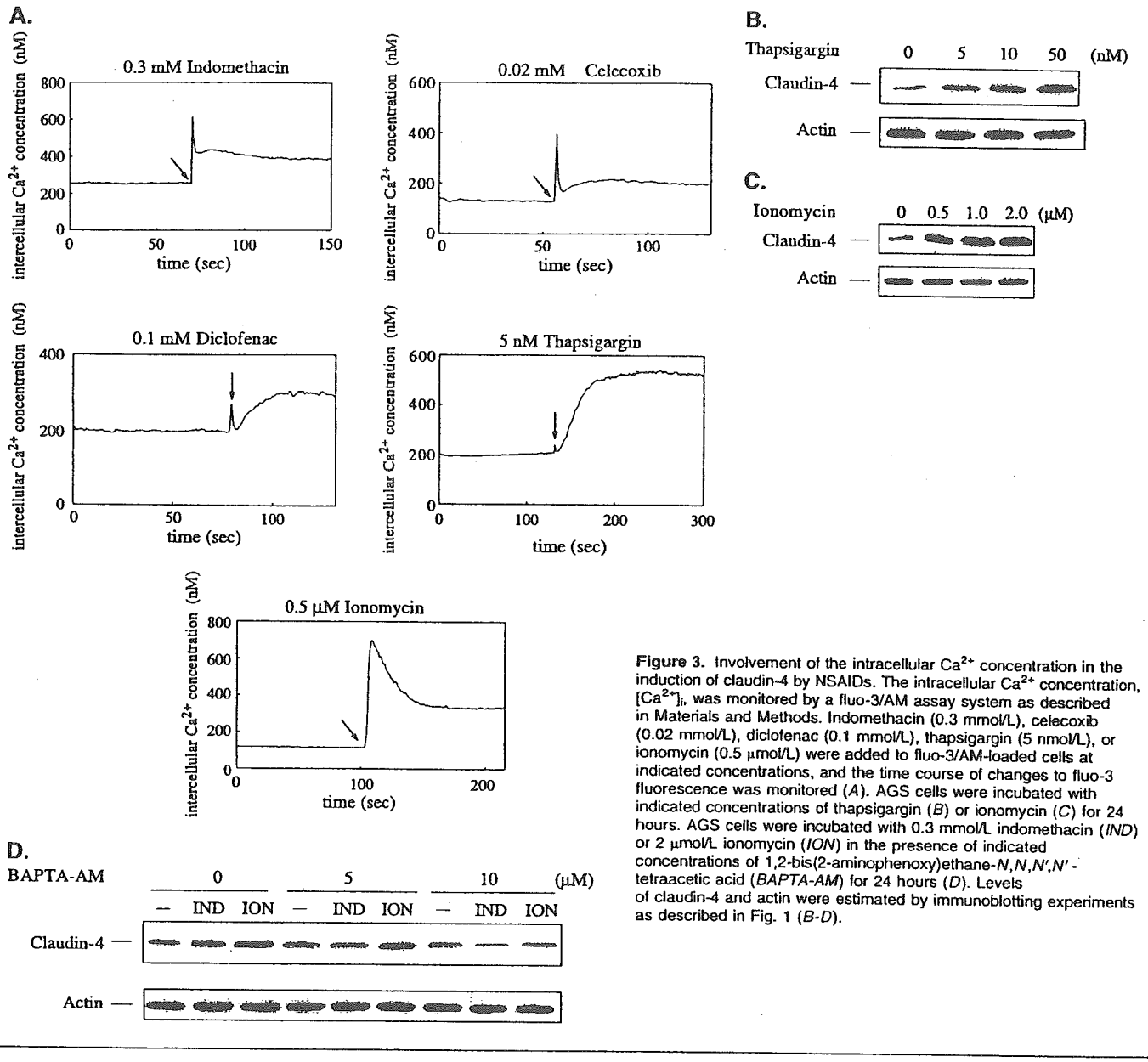

Figure 3. Involvement of the intracellular Ca^{2+} concentration in the induction of claudin-4 by NSAIDs. The intracellular Ca^{2+} concentration, $[Ca^{2+}]_i$, was monitored by a fluo-3/AM assay system as described in Materials and Methods. Indomethacin (0.3 mmol/L), celecoxib (0.02 mmol/L), diclofenac (0.1 mmol/L), thapsigargin (5 nmol/L), or ionomycin (0.5 μmol/L) were added to fluo-3/AM-loaded cells at indicated concentrations, and the time course of changes to fluo-3 fluorescence was monitored (*A*). AGS cells were incubated with indicated concentrations of thapsigargin (*B*) or ionomycin (*C*) for 24 hours. AGS cells were incubated with 0.3 mmol/L indomethacin (*IND*) or 2 μmol/L ionomycin (*ION*) in the presence of indicated concentrations of 1,2-bis(2-aminophenoxy)ethane-*N*,*N*,*N*′,*N*′-tetraacetic acid (*BAPTA-AM*) for 24 hours (*D*). Levels of claudin-4 and actin were estimated by immunoblotting experiments as described in Fig. 1 (*B-D*).

apoptosis, and inhibition of metastasis. Here, we examined the contribution that NSAID induction of claudin-4 makes to the antitumor effect of NSAIDs *in vitro*. We constructed stable transfectants of AGS cells that continuously overexpress claudin-4 and selected four clones (clones 1, 6, 7, and 11) in which the level of expression of claudin-4 varied (clone 7 > clone 11 > clone 1 > clone 6; Fig. 4*A*).

Figure 4*B* shows the cell growth curve for each clone. The growth of cells from each clone was indistinguishable from that of the mock transfectant control, demonstrating that overexpression of claudin-4 did not affect the growth of AGS cells. Therefore, induction of claudin-4 by NSAIDs does not seem to be involved in the inhibition of cell growth by NSAIDs.

We also examined the effect of overexpression of claudin-4 on the induction of apoptosis. In the absence of indomethacin, the cell viability of each clone, as determined by the trypan blue exclusion test, was close to 100%, showing that expression of claudin-4 does not affect cell viability. As shown in Fig. 4*C*, the dose-response curve for the decrease in cell viability by indomethacin was indistinguishable between each of the claudin-4-overexpressing clones and the mock transfectant control. Further, we confirmed that the cell death (Fig. 4*C*) was mediated by apoptosis as evidenced by apoptotic DNA fragmentation, activation of caspase-3, and chromatin condensation (data not shown). The results presented in Fig. 4*C* show that claudin-4 overexpression does not affect the indomethacin-induced cell apoptosis. Therefore, the induction of claudin-4 by NSAIDs does not seem to be involved in NSAID-mediated apoptosis.

The anchorage-independent growth of tumor cells, which can be measured by colony formation in soft agar, is important for tumor progression. NSAIDs are known to inhibit colony formation of some cancer cells in soft agar (13); recently, it

was reported that overexpression of claudin-4 in pancreatic cancer cells inhibited colony formation in soft agar (19). In this study, we examined the effect of claudin-4 overexpression and the presence of indomethacin on the anchorage-independent growth of AGS cells. We first examined the colony-forming ability of each of the claudin-4-overexpressing clones in soft agar. All clones showed less activity for colony formation in soft agar than the mock transfectant control (Fig. 4*D*), which is consistent with previous results obtained using pancreatic cancer cells (19). We compared the extent of inhibition of colony formation in soft agar with the degree of claudin-4 overproduction in these clones and found a close correlation between the two (Fig. 4*A* and *D*).

We also examined the effect of indomethacin on colony formation of AGS cells in soft agar. Because a long incubation period (10 days) was required for this assay, relatively low concentrations of indomethacin were used. As shown in Fig. 4*E*, indomethacin (100 μmol/L) significantly decreased the colony-forming ability of AGS cells in soft agar. Real-time RT-PCR experiments confirmed that claudin-4 mRNA expression in AGS cells was induced at the concentration of indomethacin used (Fig. 4*F*). These results suggest that the induction of claudin-4 is involved in the indomethacin-dependent inhibition of AGS cell colony formation in soft agar.

The migration activity of tumor cells is also very important for tumor progression. We examined the relationship between expression of claudin-4 and migration activity in AGS cells. Wound healing assays were carried out in which the cell-free area was measured at the time a wound was made and then 24 hours later. Because neither claudin-4 overexpression nor addition of NSAIDs affected the growth of AGS cells (Fig. 4*B*; data not shown), a smaller cell-free area is indicative of a higher activity for cell migration. As shown in Fig. 5*A*, claudin-4-overexpresing cells (clone 7) showed less cell migration activity than the mock transfectant control. Furthermore, transfection of siRNA for claudin-4 stimulated the migration activity of AGS cells even in the absence of indomethacin (Fig. 5*B*). We confirmed that the transfection almost completely inhibited the expression of claudin-4 in AGS cells (Fig. 5*C*). These results suggest that the migration activity of AGS cells decreases as claudin-4 expression increases.

As shown in Fig. 5*B*, indomethacin inhibited the activity of AGS cells for cell migration and this inhibitory effect was almost completely suppressed by the transfection of siRNA for claudin-4. We confirmed that transfection of siRNA almost completely

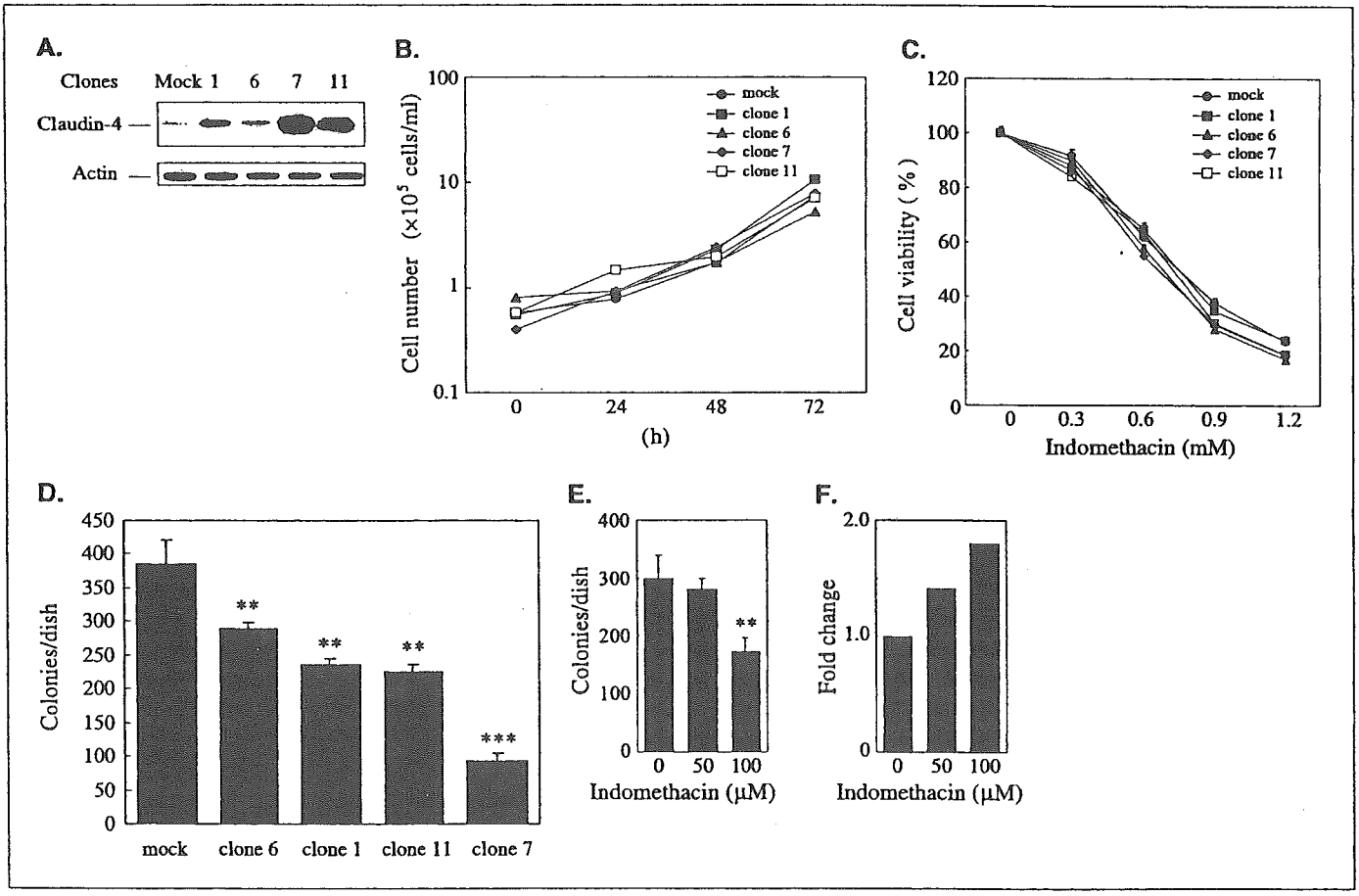

Figure 4. Effect of overexpression of claudin-4 on cell growth, apoptosis, and colony formation of AGS cells in soft agar. The extent of expression of claudin-4 in each clone (stable transfectant of claudin-4 expression plasmid) was estimated by immunoblotting experiments as described in Fig. 1 (*A*). Cells of each clone were cultured for indicated periods, and cell numbers were determined by direct cell counting (*B*). Cells of each clone were cultured in the presence of indicated concentrations of indomethacin for 24 hours and cell viability was determined by the 3-(4,5-dimethylthiazol-2-yl)-2,5-diphenyltetrazolium bromide method (*C*). Cells of each clone (*D*) or nontransfected AGS cells (*E*) were layered over soft agar in the presence (*E*) or absence (*D*) of indicated concentrations of indomethacin. After 10 days, cells were stained with crystal violet and colonies were counted (*D* and *E*). Expression of claudin-4 mRNA after treatment of cells with indicated concentrations of indomethacin for 24 hours was monitored by real-time RT-PCR (*F*). *Points*, mean ($n = 3$); *bars*, SE (*C*). *Columns*, mean (n = 3); *bars*, SE (*D and E*). ***, $P < 0.001$; **, $P < 0.01$ (*D and E*).

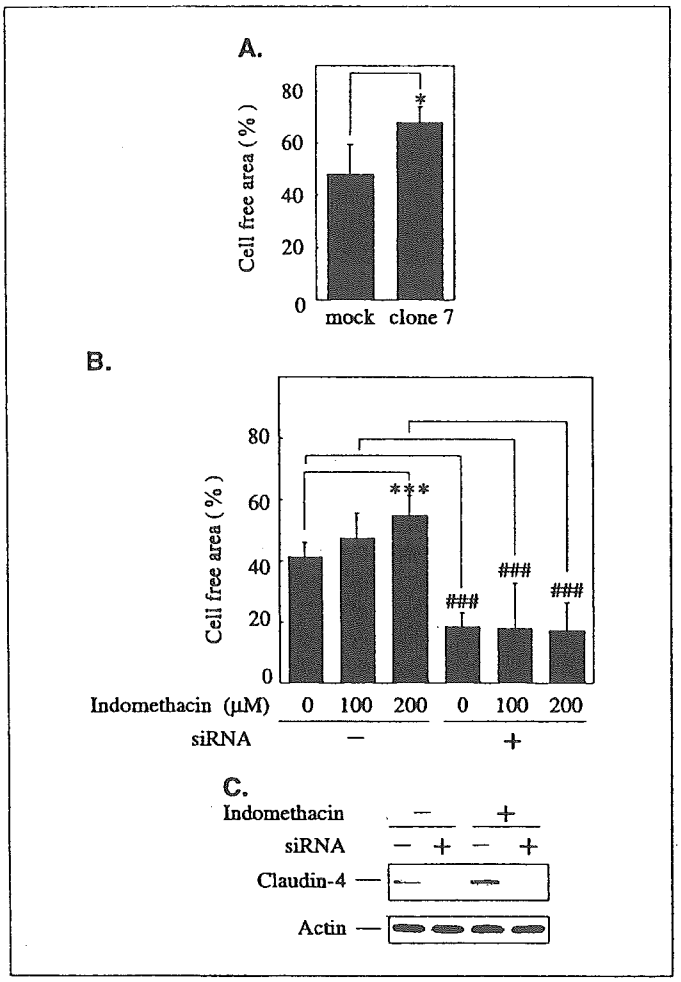

Figure 5. Effect of claudin-4 overexpression or of indomethacin on AGS cell migration. AGS cells of stable transfectant of claudin-4 expression plasmid (clone 7 in Fig. 4) and mock transfectant control AGS cells (*A*) or AGS cells transfected or nontransfected with siRNA for claudin-4 (*B*) were wounded and cultured for 24 hours in the presence (*B*) or absence (*A*) of indicated concentrations of indomethacin. The cell-free area was measured after 24 hours of incubation and expressed as relative to that before incubation. *Columns*, mean (n = 3); *bars*, SE. ***, $P < 0.001$ or ###, $P < 0.001$; *$P < 0.05$ (*A* and *B*). AGS cells transfected or nontransfected with siRNA for claudin-4 were cultured for 24 hours in the presence or absence of 0.3 mmol/L indomethacin for 24 hours. Levels of claudin-4 and actin were estimated by immunoblotting experiments as described in Fig. 1.

inhibited the induction of claudin-4 by indomethacin (Fig. 5*C*). Taken together, these results support the hypothesis that inhibition of cell migration by indomethacin is mediated through the induction of claudin-4.

Discussion

We have shown here that some tight junction–related genes, especially *claudin-4*, are induced by NSAIDs. Although NSAIDs and tight junctions are closely associated in relation to cancer progression, this is the first time that a connection between NSAIDs and tight junctions has been shown at the molecular level.

It is known that various factors disrupt or stimulate the function of tight junctions. For example, tumor necrosis factor-α, transforming growth factor-α, and interleukin-1 disrupt tight junctions, whereas transforming growth factor-β, interleukin-10, and PGE_2 are known to stimulate the function of tight junctions (41). However, the effect of these factors on the expression of components of tight junctions (such as claudin-4) has not been examined to the same extent. It seems that the alteration of tight junction function is not always correlated with an alteration in the expression of tight junction components. For example, we have found that PGE_2, which is known to stimulate the function of tight junctions, does not induce claudin-4. Because the expression of claudin-4 affects various aspects of cancer progression (see below), we consider that the effect of cancer-promoting agents or anticancer drugs on claudin-4 expression should be examined more extensively.

As for a mechanism of claudin-4 induction by NSAIDs, we postulate that it is mediated by an increase in $[Ca^{2+}]_i$ based on the following observations: (*a*) NSAIDs increased $[Ca^{2+}]_i$ and induced claudin-4 simultaneously, (*b*) thapsigargin and ionomycin increased $[Ca^{2+}]_i$ and induced claudin-4, and (*c*) the intracellular Ca^{2+} chelator [1,2-bis(2-aminophenoxy)ethane-*N*,*N*,*N*′,*N*′-tetraacetic acid] attenuated the indomethacin-dependent induction of claudin-4. As for the mechanism for the increase in $[Ca^{2+}]_i$ by NSAIDs, both inhibition of sarcoplasmic/endoplasmic reticulum Ca^{2+} ATPase (endoplasmic reticulum–located Ca^{2+} pump that is responsible for accumulation of Ca^{2+} in the endoplasmic reticulum) and stimulation of the influx of extracellular Ca^{2+} have been proposed (40). We found recently that all of the NSAIDs tested permeabilize the membranes of both erythrocytes and liposomes (42). This activity of NSAIDs was found to be closely related to their ability to increase $[Ca^{2+}]_i$, suggesting that NSAIDs permeabilize membranes and stimulate the influx of extracellular Ca^{2+} (42).

NSAIDs seem to achieve their chemopreventive effect via several mechanisms, such as stimulation of apoptosis, cell growth suppression, inhibition of angiogenesis, and inhibition of metastasis (4, 5). In this study, we examined the contribution of claudin-4 induction to the antitumor activity of NSAIDs *in vitro*. Experiments using claudin-4–overproducing AGS cells and siRNA for claudin-4 suggested that NSAID-induced claudin-4 is involved in the NSAID-dependent suppression of anchorage-independent tumor growth and tumor cell migration but not in stimulation of apoptosis and cell growth suppression. As for cell migration, this is the first evidence showing not only that NSAIDs inhibit of cancer cell migration but also that claudin-4 is involved in cell migration. It was reported recently that overexpression of claudin-4 suppressed the invasive potential of pancreatic cancer cells (19); therefore, if NSAIDs also induce claudin-4 *in vivo*, then suppression of the invasive potential of tumor cells by NSAID-induced claudin-4 may be one of the mechanisms involved in the inhibition of metastasis by NSAIDs. It is also possible that the induction of claudin-4 by NSAIDs contributes to their antitumor activity through other mechanisms. Tight junctions act as a barrier for diffusion of molecules that include nutrients and growth factors. It is well known that the constitutive accessibility of nutrients and growth factors is very important for tumor progression. Therefore, if NSAIDs also induce claudin-4 *in vivo*, then the supply of nutrients and growth factors to a tumor may be retarded or inhibited, thereby suppressing tumor progression.

Acknowledgments

Received 8/3/2004; revised 11/22/2004; accepted 12/20/2004.

Grant support: Ministry of Health, Labor, and Welfare of Japan Grants-in-Aid for Scientific Research, Suzuken Memorial Foundation, and Japan Research Foundation for Clinical Pharmacology.

The costs of publication of this article were defrayed in part by the payment of page charges. This article must therefore be hereby marked advertisement in accordance with 18 U.S.C. Section 1734 solely to indicate this fact.

References

1. Smalley WE, Ray WA, Daugherty JR, Griffin MR. Nonsteroidal anti-inflammatory drugs and the incidence of hospitalizations for peptic ulcer disease in elderly persons. Am J Epidemiol 1995;141:539–45.
2. Farrow DC, Vaughan TL, Hansten PD, et al. Use of aspirin and other nonsteroidal anti-inflammatory drugs and risk of esophageal and gastric cancer. Cancer Epidemiol Biomarkers Prev 1998;7:97–102.
3. Sorensen HT, Friis S, Norgard B, et al. Risk of cancer in a large cohort of nonaspirin NSAID users: a population-based study. Br J Cancer 2003;88:1687–92.
4. Gupta RA, Dubois RN. Colorectal cancer prevention and treatment by inhibition of cyclooxygenase-2. Nat Rev Cancer 2001;1:11–21.
5. Kismet K, Akay MT, Abbasoglu O, Ercan A. Celecoxib: a potent cyclooxygenase-2 inhibitor in cancer prevention. Cancer Detect Prev 2004;28:127–42.
6. Hoshino T, Tsutsumi S, Tomisato W, Hwang HJ, Tsuchiya T, Mizushima T. Prostaglandin E_2 protects gastric mucosal cells from apoptosis via EP2 and EP4 receptor activation. J Biol Chem 2003;278:12752–8.
7. Tsuji M, Kawano S, Tsuji S, Sawaoka H, Hori M, DuBois RN. Cyclooxygenase regulates angiogenesis induced by colon cancer cells. Cell 1998;93:705–16.
8. Rolland PH, Martin PM, Jacquemier J, Rolland AM, Toga M. Prostaglandin in human breast cancer: evidence suggesting that an elevated prostaglandin production is a marker of high metastatic potential for neoplastic cells. J Natl Cancer Inst 1980;64:1061–70.
9. Eberhart CE, Coffey RJ, Radhika A, Giardiello FM, Ferrenbach S, DuBois RN. Up-regulation of cyclooxygenase 2 gene expression in human colorectal adenomas and adenocarcinomas. Gastroenterology 1994;107:1183–8.
10. Ristimaki A, Honkanen N, Jankala H, Sipponen P, Harkonen M. Expression of cyclooxygenase-2 in human gastric carcinoma. Cancer Res 1997;57:1276–80.
11. Piazza GA, Alberts DS, Hixson LJ, et al. Sulindac sulfone inhibits azoxymethane-induced colon carcinogenesis in rats without reducing prostaglandin levels. Cancer Res 1997;57:2909–15.
12. Reddy BS, Kawamori T, Lubet RA, Steele VE, Kelloff GJ, Rao CV. Chemopreventive efficacy of sulindac sulfone against colon cancer depends on time of administration during carcinogenic process. Cancer Res 1999;59:3387–91.
13. Zhang X, Morham SG, Langenbach R, Young DA. Malignant transformation and antineoplastic actions of nonsteroidal antiinflammatory drugs (NSAIDs) on cyclooxygenase-null embryo fibroblasts. J Exp Med 1999;190:451–9.
14. Hanif R, Pittas A, Feng Y, et al. Effects of nonsteroidal anti-inflammatory drugs on proliferation and on induction of apoptosis in colon cancer cells by a prostaglandin-independent pathway. Biochem Pharmacol 1996;52:237–45.
15. Anderson JM, Van Itallie CM. Tight junctions and the molecular basis for regulation of paracellular permeability. Am J Physiol 1995;269:G467–5.
16. Soler AP, Miller RD, Laughlin KV, Carp NZ, Klurfeld DM, Mullin JM. Increased tight junctional permeability is associated with the development of colon cancer. Carcinogenesis 1999;20:1425–31.
17. Li D, Mrsny RJ. Oncogenic Raf-1 disrupts epithelial tight junctions via downregulation of occludin. J Cell Biol 2000;148:791–800.
18. Hoevel T, Macek R, Swisshelm K, Kubbies M. Reexpression of the TJ protein CLDN1 induces apoptosis in breast tumor spheroids. Int J Cancer 2004;108:374–83.
19. Michl P, Barth C, Buchholz M, et al. Claudin-4 expression decreases invasiveness and metastatic potential of pancreatic cancer. Cancer Res 2003;63:6265–71.
20. Baek SJ, Kim KS, Nixon JB, Wilson LC, Eling TE. Cyclooxygenase inhibitors regulate the expression of a TGF-β superfamily member that has proapoptotic and antitumorigenic activities. Mol Pharmacol 2001;59:901–8.
21. Tsutsumi S, Gotoh T, Tomisato W, et al. Endoplasmic reticulum stress response is involved in nonsteroidal anti-inflammatory drug-induced apoptosis. Cell Death Differ 2004;11:1009–16.
22. Tsutsumi S, Tomisato W, Hoshino T, Tsuchiya T, Mizushima T. Transforming growth factor-β1 is responsible for maturation-dependent spontaneous apoptosis of cultured gastric pit cells. Exp Biol Med (Maywood) 2002;227:402–11.
23. Tsutsumi S, Tomisato W, Takano T, Rokutan K, Tsuchiya T, Mizushima T. Gastric irritant-induced apoptosis in guinea pig gastric mucosal cells in primary culture. Biochim Biophys Acta 2002;1589:168–80.
24. Kao JP, Harootunian AT, Tsien RY. Photochemically generated cytosolic calcium pulses and their detection by fluo-3. J Biol Chem 1989;264:8179–84.
25. Wittchen ES, Haskins J, Stevenson BR. ZO-3 expression causes global changes to actin cytoskeleton in Madin-Darby canine kidney cells: linking a tight junction protein to Rho GTPases. Mol Biol Cell 2003;14:1757–68.
26. Ciardiello F, Caputo R, Damiano V, et al. Antitumor effects of ZD6474, a small molecule vascular endothelial growth factor receptor tyrosine kinase inhibitor, with additional activity against epidermal growth factor receptor tyrosine kinase. Clin Cancer Res 2003;9:1546–56.
27. Bottone FG Jr, Martinez JM, Collins JB, Afshari CA, Eling TE. Gene modulation by the cyclooxygenase inhibitor, sulindac sulfide, in human colorectal carcinoma cells: possible link to apoptosis. J Biol Chem 2003;278:25790–801.
28. Rahner C, Mitic LL, Anderson JM. Heterogeneity in expression and subcellular localization of claudins 2, 3, 4, and 5 in the rat liver, pancreas, and gut. Gastroenterology 2001;120:411–22.
29. Lim JW, Kim H, Kim KH. Nuclear factor-κB regulates cyclooxygenase-2 expression and cell proliferation in human gastric cancer cells. Lab Invest 2001;81:349–60.
30. Fan XM, Wong BC, Lin MC, et al. Interleukin-1β induces cyclo oxygenase-2 expression in gastric cancer cells by the p38 and p44/42 mitogen-activated protein kinase signaling pathways. J Gastroenterol Hepatol 2001;16:1098–104.
31. Tsuji S, Kawano S, Sawaoka H, et al. Evidences for involvement of cyclooxygenase-2 in proliferation of two gastrointestinal cancer cell lines. Prostaglandins Leukot Essent Fatty Acids 1996;55:179–83.
32. Tsujii M, Kawano S, DuBois RN. Cyclooxygenase-2 expression in human colon cancer cells increases metastatic potential. Proc Natl Acad Sci U S A 1997;94:3336–40.
33. Merritt G, Aliprandis ET, Prada F, Rigas B, Kashfi K. The retinoid fenretinide inhibits proliferation and downregulates cyclooxygenase-2 gene expression in human colon adenocarcinoma cell lines. Cancer Lett 2001;164:15–23.
34. Kawai S, Nishida S, Kato M, et al. Comparison of cyclooxygenase-1 and -2 inhibitory activities of various nonsteroidal anti-inflammatory drugs using human platelets and synovial cells. Eur J Pharmacol 1998;347:87–94.
35. Lehmann JM, Lenhard JM, Oliver BB, Ringold GM, Kliewer SA. Peroxisome proliferator activated receptors α and γ are activated by indomethacin and other nonsteroidal anti-inflammatory drugs. J Biol Chem 1997;272:3406–10.
36. Huang JT, Welch JS, Ricote M, et al. Interleukin-4-dependent production of PPAR-γ ligands in macrophages by 12/15-lipoxygenase. Nature 1999;400:378–82.
37. Kusuhara H, Komatsu H, Sumichika H, Sugahara K. Reactive oxygen species are involved in the apoptosis induced by nonsteroidal anti-inflammatory drugs in cultured gastric cells. Eur J Pharmacol 1999;383:331–7.
38. Elder DJ, Halton DE, Playle LC, Paraskeva C. The MEK/ERK pathway mediates COX-2-selective NSAID-induced apoptosis and induced COX-2 protein expression in colorectal carcinoma cells. Int J Cancer 2002;99:323–7.
39. Tepperman BL, Soper BD. Effect of extracellular Ca^{2+} on indomethacin-induced injury to rabbit dispersed gastric mucosal cells. Can J Physiol Pharmacol 1994;72:63–9.
40. Wang JL, Lin KL, Chen JS, et al. Effect of celecoxib on Ca^{2+} movement and cell proliferation in human osteoblasts. Biochem Pharmacol 2004;67:1123–30.
41. Sawada N, Murata M, Kikuchi K, et al. Tight junctions and human diseases. Med Electron Microsc 2003;36:147–56.
42. Tomisato W, Tanaka K, Katsu T, et al. Membrane permeabilization by non-steroidal anti-inflammatory drugs. Biochem Biophys Res Commun 2004;323:1032–9.

Digestive Diseases and Sciences, Vol. 50, No. 9 (September 2005), pp. 1641–1646 (c 2005)
DOI: 10.1007/s10620-005-2909-x

Low Direct Cytotoxicity of Nabumetone on Gastric Mucosal Cells

YASUHIRO ARAI, BS,* KEN-ICHIRO TANAKA, BS,* HIRONORI USHIJIMA, BS,* WATARU TOMISATO, PhD,† SHINJI TSUTSUMI, PhD,* MAYUKO ABURAYA, BS,* TATSUYA HOSHINO, BS,* KAZUMI YOKOMIZO, PhD,* KEITAROU SUZUKI, PhD,* TAKASHI KATSU, PhD,† TOMOFUSA TSUCHIYA, PhD,† and TOHRU MIZUSHIMA, PhD*

Prodrugs of non-steroidal anti-inflammatory drugs (NSAIDs) are widely used for clinical purposes because they are not harmful to the gastrointestinal mucosa. We recently showed that NSAIDs have direct cytotoxicity in NSAID-induced gastric lesions. We show here that under conditions where the NSAIDs indomethacin and celecoxib clearly induce cell death, an NSAID prodrug, nabumetone, and its active metabolite 6-methoxy-2-naphthylacetic acid (6MNA), did not have such effects. Moreover, nabumetone and 6MNA exhibited much lower membrane permeabilizing activities than did indomethacin and celecoxib. We recently reported that when an orally administered NSAID was used in combination with a low dose of intravenously administered indomethacin, the severity of gastric lesions produced in rats depended on the cytotoxicity of the orally administered NSAID. Using a similar protocol, we show here that gastric lesions were produced when the orally administered NSAID was celecoxib, but not when nabumetone was used. We thus propose that the low direct cytotoxicity of nabumetone observed in vitro is maintained in vivo, and that the use of nabumetone does not harm the gastric mucosa.

KEY WORDS: nabumetone; gastric mucosal cells; membrane permeabilization; gastric lesions.

Non-steroidal anti-inflammatory drugs (NSAIDs) are very popular and effective medicines used in the treatment of pain, inflammation and fever. The anti-inflammatory action of NSAIDs is mediated by their inhibition of cyclooxygenase (COX) activity. COX is an enzyme that is essential for the synthesis of prostaglandins (PGs), which have a strong capacity to induce inflammation. On the downside, the use of NSAIDs is associated with gastrointestinal side-effects (1), with about 15–30% of chronic users of NSAIDs suffering from gastrointestinal ulcers and bleeding (2, 3). This negative aspect of NSAID use was previously thought to be due only to the inhibition of COX, because PGs have a strong protective effect on the gastrointestinal mucosa (4). In order to overcome the gastrointestinal side-effects of NSAID use, NSAIDs that inhibit COX activity in inflammatory tissues but not in the gastric mucosa are therefore required. Selective COX-2 inhibitors belong to such a category of NSAIDs. COX has two subtypes, COX-1 and COX-2, which are responsible for the majority of COX activity in the gastric mucosa and in inflamed tissues, respectively (5, 6). While a greatly reduced incidence of gastroduodenal lesions was reported for selective COX-2 inhibitors (such as rofecoxib and celecoxib) both in animal and clinical data (7, 8), their use however has been recently questioned because of their potential for causing cardiovascular thrombotic events owing to their specificity for COX-2 (9–12).

Manuscript received November 7, 2004; accepted January 12, 2005.

From the *Graduate School of Medical and Pharmaceutical Sciences, Kumamoto University, Kumamoto 862-0973, and †Faculty of Pharmaceutical Sciences, Okayama University, Okayama 700-8530, Japan.

This work was supported by Grants-in-Aid for Scientific Research from the Ministry of Health, Labour, and Welfare of Japan, as well as by the Suzuken Memorial Foundation, and the Japan Research Foundation for Clinical Pharmacology.

Address for reprint requests: Dr. Tohru Mizushima, Graduate School of Medical and Pharmaceutical Sciences, Kumamoto University, Kumamoto 862-0973, Japan; mizu@gpo.kumamoto-u.ac.jp.

NSAID prodrugs (such as loxoprofen sodium and nabumetone) are generally safe for use on the gastrointestinal mucosa and are widely used for clinical purposes, especially in Japan where highly specific COX-2 inhibitors (such as celecoxib) are not presently available in the market. Because most NSAID prodrugs do not possess any significant specificity for COX-2, these prodrugs may become very important as NSAIDs, considering the potential risk for cardiovascular thrombotic events of selective COX-2 inhibitors.

NSAIDs have a direct cytotoxic effect on gastrointestinal mucosal cells (13, 14) and we recently demonstrated that NSAIDs induce both necrosis and apoptosis in cultured gastric mucosal cells in a manner independent of COX inhibition (15–17). We also found that NSAIDs cause membrane permeabilization, which in turn is implicated in their direct cytotoxicity; that is, liposomal membranes are directly permeabilized by NSAIDs at concentrations closely related to those which result in cytotoxicity (18). Furthermore, we recently suggested that the combined effect of COX inhibition and the direct cytotoxic effect of NSAIDs (direct cell damage) on the gastric mucosa induces the production of gastric lesions (19). Therefore, the direct cytotoxicity of individual NSAIDs is a key factor to be determined in assessing their harmfulness on the gastric mucosa.

Since the direct cytotoxicity of NSAID prodrugs has not been studied at all, we examined here the direct cytotoxicity of nabumetone which, along with its active metabolite 6-methoxy-2-naphthylacetic acid (6MNA), was found to not harm the gastrointestinal mucosa in clinical studies on humans and in animal models (20, 21). Compared to indomethacin and celecoxib, both nabumetone and 6MNA showed very low activities for inducing necrosis, apoptosis and membrane permeabilization. Furthermore, in combination with the intravenous administration of a low dose of indomethacin (conditions under which gastric mucosal COX activity is completely inhibited), the oral administration of nabumetone did not result in the production of gastric lesions, which is in contrast to results obtained following the oral administration of celecoxib. Based on these observations, we consider that the low direct cytotoxicity of nabumetone will render its use safe on the gastrointestinal mucosa in vivo.

MATERIALS AND METHODS

Chemicals and Media. Fetal bovine serum (FBS) was from Gibco Co. 3-(4, 5-dimethyl-thiazol-2-yl)-2,5-diphenyl tetrazolium bromide (MTT) was from Sigma Co. Nabumetone and 6MNA were kindly gifted from Sanwa Kagaku Kenkyusho Co. Indomethacin was from Wako Co. Celecoxib was from LKT Laboratories Inc. Egg phosphatidylcholine (PC) was from Kanto Chemicals Co. The ELISA kit for PGE_2 quantitation was from Cayman Chemical Co. Male Wistar rats weighing 160–200 g and male guinea pigs weighing 200–300 g were purchased from Shimizu Co. The experiments and procedures described here were carried out in accordance with the Guide for the Care and Use of Laboratory Animals as adopted and promulgated by the National Institute of Health and were approved by the Animal Care Committee of Kumamoto University.

In Vitro Assay of Cytotoxicity of NSAIDs

Gastric mucosal cells were isolated from guinea pig fundic glands as described previously (22, 23). Isolated gastric mucosal cells were cultured for 12 hr in RPMI 1640 containing 0.3% v/v FBS, 100 U/ml ampicillin and 100 μg/ml streptomycin in type-I collagen-coated plastic culture plates under the conditions of 5% CO_2/95% air and 37 C. After removing non-adherent cells, cells attached to the plate were used. Guinea pig gastric mucosal cells prepared under these conditions were previously characterized, with the majority (about 90%) of cells being identified as pit cells (22, 24).

NSAIDs were dissolved in DMSO. Cells were exposed to NSAIDs by changing the entire bathing medium.

We used MTT assay for monitoring cell viability. Cells were incubated for 2 hr with MTT solution at a final concentration of 0.5 mg/ml. Isopropanol and hydrochloric acid were added to the culture medium at final concentrations of 50% and 20 mM, respectively. The optical density of each sample at 570 nm was determined spectrophotometrically using a reference wavelength of 630 nm (25).

Gastric Damage Assay. Gastric damage assays were performed as described previously (19). Rats (24 hr fasted) were administered orally with NSAIDs in 1% methylcellulose in a volume of 5 ml/kg. In some experiments, indomethacin in PBS was administered intravenously 1 hr before the oral administration. Six hours after the oral administration, the rats were anesthetized and the stomach was removed and scored for hemorrhagic damage by an observer unaware of the treatment the rats had received. The score involved measuring the area of all lesions in millimeters squared and summing the values to give an overall gastric lesion index. Determination of PGE_2 levels at the gastric mucosa was done by ELISA as previously described (26).

Assay for Erythrocyte Hemolysis. Hemolysis in erythrocytes were monitored as described (18). Human erythrocytes were washed twice with buffer A (5 mM HEPES/NaOH (pH 7.4) and 150 mM NaCl) and then suspended in fresh buffer A at a final concentration of 0.5% hematocrit (5×10^7 cells/ml). After incubation with NSAIDs for 10 min at 30 C, hemolysis was estimated by measuring the absorbance at 540 nm.

Membrane Permeability Assay. Membrane permeability assays were performed as described previously (18). Liposomes were prepared using the reversed-phase evaporation method. Egg PC (10 μmol, 7.7 mg) was dissolved in chloroform/methanol (1:2, v/v), dried, and dissolved in 1.5 ml of diethyl ether. This was followed by the addition of 1 ml of 100 mM calcein-NaOH (pH 7.4). The mixture was sonicated to obtain a homogenous emulsion. The diethyl ether solvent was removed using a conventional rotary evaporator under reduced pressure at 25 C. The resulting suspension of liposome was centrifuged and washed twice with fresh buffer A (10 mM phosphate buffer, containing 150 mM NaCl) to remove untrapped calcein. The final liposome